2012

Soil Accretion and Organic Carbon Accumulation in the Tidal Salt Marshes of the Liaohe Delta, China

Nicholas Lawrence Yuknis
Louisiana State University and Agricultural and Mechanical College

SOIL ACCRETION AND ORGANIC CARBON ACCUMULATION IN THE TIDAL SALT MARSHES OF THE LIAOHE DELTA, CHINA

A Thesis

Submitted to the Graduate Faculty of the
Louisiana State University and
Agricultural and Mechanical College
in partial fulfillment of the
requirements for the degree of
Master of Science

In

The Department of Environmental Sciences

by
Nicholas Yuknis
B.S.P.A., Indiana University, Bloomington, May 2009
May 2012

ACKNOWLEDGEMENTS

Funding for this project was jointly provided by the National Natural Science Foundation of China (grant number 40872167) and the Ministry of Land and Resources Program: "special foundation for scientific research on public causes" (grant number 201111023). Without this funding, this research would not have been possible.

I would like to sincerely thank my advisors Drs. Ed Laws, Andy Nyman, and Aixin Hou for their guidance throughout this entire experience. I truly appreciate all of the time and hard work they committed to making this project and thesis a success.

I appreciate all that my host professors Drs. Siyuan Ye and Chunding Xue have done for me while in China and after I left. They guided me through my research and provided helpful suggestions during sampling and sample analysis that led to the successful completion of this project. No matter how difficult or frustrating the issues were at hand, they continuously reassured me that "these issues always happen in research" and "do not worry, this project will be a success in the end," which gave me confidence in my abilities and results. In addition to their help with research, they were the best hosts I could have asked for; they made me feel extremely comfortable while abroad and exposed me to the beautiful and unique culture of China that a casual tourist would otherwise miss. Additionally, this project would not have been possible, or as enjoyable, without the help and company of all the graduate students and research associates I worked with in China. They made this an unforgettable and fun experience. Thank you Xigui, Guangming, Hongming, Ellen, Miao, Xue Yang, and Qingyuan.

Lastly, I would like to thank my family for their constant support throughout my tenure at LSU, but especially during my trip to China. I love you all and know you will always be there for me when I need you, no matter how difficult the circumstance.

TABLE OF CONTENTS

LIST OF TABLES

LIST OF FIGURES

ABSTRACT

Wetlands provide a multitude of functions to people and ecosystems and because of this, maintaining or increasing wetland area is important. Wetlands can be significant carbon sinks because of the relatively high primary productivity and slow decomposition of organic matter in these systems and can thus impact the global carbon cycle and potentially climate change. The marshes of the Liaohe Delta are the largest in Liaoning Province; however, very little research has been done in this area to determine the rate of accretion and organic carbon sequestration in the salt marshes there. By using ^{137}Cs and ^{210}Pb dating techniques and organic matter combustion, I analyzed nine cores to determine accretion and organic carbon accumulation rates in three vegetation density treatments of *Suaeda salsa* (mudflat, half cover, full cover) and at different marsh elevations. Results from ^{137}Cs analysis showed no cores with a distinctive peak at depth that might have corresponded to the peak fallout year of ^{137}Cs (1963) or a depth at which ^{137}Cs activity was undetectable (pre-1954). Accretion rates were estimated to be greater than 1.09 cm yr^{-1} at all sites based on ^{137}Cs techniques, from 0.85 to 9.73 cm yr^{-1} at all sites based on ^{210}Pb techniques combined with the c.r.s. and c.f.:c.s. models, and were highest at the two sites below sea level. Organic carbon accumulation rates ranged from 137 to 1,522 g m^{-2} yr^{-1} at all sites and were highest at the two sites below sea level. No differences in accretion or organic carbon accumulation were found among different vegetation density treatments; however, accretion and organic carbon accumulation were significantly greater at sites below sea level ($p <$ 0.02). It is likely that lower elevation sites were inundated for longer periods of time, which would provide greater opportunity for suspended sediment deposition. Higher organic carbon accumulation rates at sites resulted from increased accretion with similar percent organic carbon. Additional research is needed to provide insight on the accuracy of calculated accretion and OC

accumulation rates from this study and proper application of ^{210}Pb dating models on salt marshes in this region.

1. INTRODUCTION

Wetlands provide a multitude of significant functions to people and ecosystems and because of this, maintaining or increasing wetland area is important. Some of these functions include storing water, providing habitat, transforming chemical species, and acting as a source or sink for nutrients. Wetlands can be significant carbon sinks because of the relatively high primary productivity and slow decomposition of organic matter in these temporarily or permanently flooded systems (Dring 1982, Nyman and DeLaune 1991). Wetland soils (histosols) have the highest organic carbon concentration of any soil unit, the global average being 77.6 kg m^{-2} in the upper 100 cm (Batjes 1996). In addition, wetlands are estimated to store about 20 to 30 percent of the total global terrestrial carbon in their soils (Mitsch and Gosselink 2007), even though they only occupy about 5 to 8 percent of the land surface on Earth (Aselmann and Crutzen 1989, Lehner and Doll 2004, Mitsch and Gosselink 2007).

Accretion is the vertical increase in the elevation of the soil surface in cm yr^{-1} and is usually controlled to some extent by elevation, vegetation, and sediment supply. Salt marshes with lower elevations are typically flooded more frequently than higher elevation marshes, which may provide a greater opportunity for suspended sediment deposition (Cahoon and Reed 1995, Chmura et al. 2001); salt marshes with greater vegetation density have a greater ability to trap sediment (Rooth and Stevenson 2000, Yang and Chen 1995) or accrete via organic deposition (McCaffrey and Thomson 1980, Nyman et al. 2006). Identifying accretion rates in coastal marshes can help researchers understand the potential effects of sea level rise on wetland loss and understand the rate at which wetlands are being created. Furthermore, quantifying carbon pools and carbon accumulation rates in different ecosystems is important because carbon plays a large role in global climate change. Much work has been done on estimating accretion rates and

carbon storage in fresh and salt marshes around the world (Bao et al. 2011, Chmura et al. 2003, Craft and Richardson 1998, Gorham 1991, Nyman et al. 2006); however, very little is known about these processes in the coastal salt marshes of the Liaohe Delta, China. Conservation of these marshes is a priority because they provide important breeding and wintering habitat for at least 116 species of migratory birds, including the endangered Red-crowned Crane and threatened Saunder's Gull (Liu et al. 2000, Scott 1989); in addition, they support crab and shrimp fisheries that provide financial sustenance to local residents (Duning et al. 1996).

The purpose of this study was to estimate recent accretion rates and organic carbon accumulation rates at sites characterized by three vegetation density treatments (mudflat, half cover, full cover) and at different elevations in the tidal salt marshes of the Liaohe Delta, Northeast China. Soil cores within each treatment were analyzed for ^{137}Cs, ^{210}Pb, ^{226}Ra, and organic matter content to determine accretion rates and accumulation rates from nine sampling locations. Results from this project should provide a better understanding of soil accretion and organic carbon accumulation processes at different elevations and vegetation densities in the Liaohe Delta. It was hypothesized that accretion and organic carbon accumulation rates would be greatest in the highest vegetation density treatment and lower elevation sites because of potentially higher soil deposition caused by increased organic matter production and inundation duration at those sites.

2. LITERATURE REVIEW

2.1 Wetlands and Carbon Storage

Wetlands have a wide range of carbon storage potential that largely depends on wetland type and location. Chmura et al. (2003) reported global C sequestration rates averaging 210 ± 20 g organic carbon (OC) m^{-2} yr^{-1} with a range from 17 to 1713 g OC m^{-2} yr^{-1} in tidal saline wetlands. The high variability of C storage in these wetlands has been attributed to local and regional differences in suspended sediment supply, mean annual temperature, and tidal flooding (Chmura et al. 2003). Global and regional C sequestration rate estimates for peatlands and prairie pothole wetlands have been reported to range from 20 to 30 g C m^{-2} yr^{-1} and 83 to 305 g OC m^{-2} yr^{-1}, respectively (Roulet 2000, Euliss et al. 2006). While C sequestration rates in some saline and freshwater marshes are similar, decomposition in freshwater marshes commonly results in high CH_4 fluxes to the atmosphere (Mitsch and Wu 1995). Because CH_4 has a greater ability to absorb infrared radiation than CO_2 on a molecular basis, increased methane emissions may reduce many of the benefits C storage provides in freshwater marshes with respect to climate change mitigation (Whiting and Chanton 2001). Freshwater marshes have the ability to contribute a substantial amount of CH_4 to the atmosphere; prior to the anthropocene era, terrestrial wetlands have been estimated to account for as much as 76% of CH_4 emissions to the atmosphere (Beerling et al. 2009). The presence of SO_4 in salt water and preferential use of SO_4 as the terminal electron acceptor to CO_2 during microbial oxidation of organic matter prevents much CH_4 from being produced in salt marshes (DeLaune et al. 1983, Mitsch and Wu 1995).

2.2 Soil Accretion

The maintenance and creation of coastal wetlands is largely governed by a combination of processes that change the elevation and hydroperiod of the soil (Figure 2.1). Factors that

increase submergence include subsidence and sea level rise, whereas soil accretion decreases submergence (Nyman et al. 1993b). If soil accretion is greater than sea level rise and subsidence, then the coastal wetland is emerging. Conversely, if soil accretion is less than sea level rise and subsidence, then the coastal wetland is submerging. Soil accretion results from the addition of two types of soil material: inorganic (mineral material) and organic material (Nyman et al. 2006, Reed 1995, Rooth et al. 2003). Vertical accretion in coastal wetland soils is most commonly described as being dependent on inorganic deposition and less commonly dependent on organic matter deposition to maintain or increase soil elevation (Nyman et al. 1990, Reed 1990, Temmerman et al. 2004). The degree of inorganic deposition is controlled by the depth and duration of inundation of the marsh surface and availability of inorganic material, all of which can be influenced by marsh elevation, sea level rise, rivers, tides, and storm events (Reed 1989, 1990; Rejmanek et al. 1988). The degree of organic matter deposition is controlled by aboveground and belowground biomass production and deposition (Nyman et al. 2006, Rooth and Stevenson 2000, Wolaver et al. 1988). The inorganic and organic components are typically and primarily derived from allochthonous (originating from another location) and autochthonous (originating from the same location) sources, respectively (French 2006).

The rate of soil accretion is also controlled by inundation, sediment supply, and vegetation. The single species model proposed by Morris (2007) describes the effect of sea level rise on accretion rates in salt marshes as being primarily controlled by soil inundation depth, suspended sediment concentration, and vegetation density. In this model, soil accretion is maximized when soil inundation depth is at an optimum level for plant productivity, assuming this depth is below the mean high tide (Morris 2007). However, an inundation depth that reduces productivity will limit a plant's ability to trap sediment and deposit organic matter (Morris 2007).

Similarly, a marsh elevation that is near the mean high tide will have limited suspended sediment load and settling time because of decreased inundation depth and duration, which will likely result in lower inorganic deposition (Morris 2007). Different salt marshes may have a larger or smaller suspended sediment supply, which would decrease or increase the impact of vegetation on accretion, respectively.

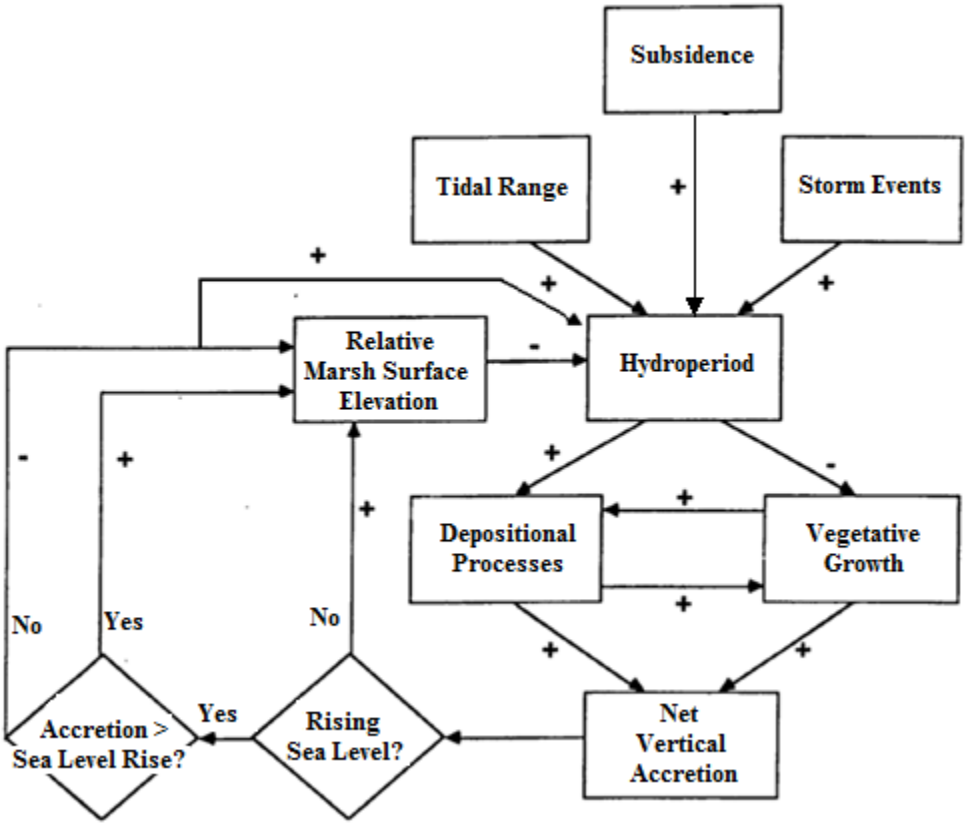

Figure 2.1: The interaction of sea-level rise, subsidence, hydroperiod, depositional, and vegetative processes controlling vertical accretion of coastal marshes. Pluses and minuses indicate an increase and decrease in the following process resulting from the previous process, respectively. Adapted from Reed (1990).

2.3 Inorganic Accumulation Processes

Inorganic accumulation rate is defined as the mass of inorganic accumulation in g m^{-2} yr^{-1}. Inorganic accumulation requires a combination of flooded soils and inorganic sediment availability (Reed 1989). In the short term, the level of soil inundation and inorganic deposition

is determined by the tidal range and elevation of the marsh (Collins et al. 1987, Reed 1990). However, over long periods of time, sea level rise and subsidence can increase the duration and depth of soil inundation if vertical accretion cannot keep pace with these processes (Reed 1990). This can result in the death of vegetation because of excessive flooding and salt stress (Boesch et al. 1994). Vegetation is important in inorganic accumulation because live vegetation and litter can trap sediment (Rooth and Stevenson 2000, Yang and Chen 1995). Different plant species have been shown to be more effective than others at trapping sediment. In a study from the Chesapeake Bay, Rooth and Stevenson (2000) determined that 245 g m^{-2} of sediment were deposited in a *Phragmites australis* community, whereas less than 30% of that (< 73.5 g m^{-2}) was deposited in a *Spartina* spp. community during a large storm event. This effect was attributed to increased vegetative cover and litter in the *P. australis* wetland community (Rooth and Stevenson 2000). In addition, vegetation acts as a mechanism to slow the flow of water, which allows suspended sediment to settle (Yang and Chen 1995).

2.4 Organic Accumulation Processes

Organic accumulation rate is defined as the mass of organic accumulation in g m^{-2} yr^{-1}. Organic accumulation is a complex process, as it involves the interaction of soil hydroperiods, inorganic input, salinity, redox potential (Eh), temperature, and vegetation type. These parameters control the production, transport, and decomposition of organic material. Organic matter is deposited in the soil from both aboveground and belowground biomass (Reed 1995). However, in order for autochthonous organic accumulation to be initiated, favorable conditions for rooted macrophyte growth must be present. Inorganic deposition may create favorable conditions by increasing elevation to a point that flood stress no longer prevents macrophyte plant growth. This process is evident in the progradation portion of the delta cycle, as described

by Roberts (1997). Once plant growth is established, primary production is usually very high in salt marshes, but varies depending on vegetation type, salinity, location, and hydroperiod (Howes et al. 1985, Windham 2001). Primary production can be limited by a variety of stressors; some of these stressors include high salt concentrations, extended hydroperiods, and presence of toxic ions (Koch and Mendelssohn 1989, Reed 1995). This decreased productivity would limit the amount of autochthonous organic matter available for deposition. Tidal flooding or storm events can also act as a means to deposit allochthonous organic material in an adjacent marsh (Reed 1995). Inorganic input can enhance primary productivity via deposition of nutrients associated with inorganic sediment, such as sediment-bound NH_4 or associated particulate organic N and P (DeLaune et al. 1981a, Liu et al. 2008a, McLatchey and Reddy 1998). Nutrients bound in organic matter can become available to vegetation during the mineralization of organic matter, which is largely controlled by the rate of decomposition (McLatchey and Reddy 1998). Vegetation can also contribute to accretion and organic accumulation and combat excessive flooding caused by sea level rise and subsidence through the production of adventitious root structures (aquatic roots) above the soil surface in flooded conditions. This process is evident in some *Spartina alterniflora* and *Spartina patens* marshes in coastal Louisiana and Connecticut (McCaffrey and Thomson 1980, Nyman et al. 2006).

2.4.1 Plant Stressors

Flooding and salinity are two major stressors that limit salt marsh plant growth. Excessive flooding can restrict growth by limitation of nutrient uptake and through the production and accumulation of phytotoxins. Flooded conditions may cause root oxygen deficiency, which can increase root anaerobic respiration, resulting in less ATP production and limited NH_4 uptake in some salt marsh species (Koch et al. 1990). If soils are flooded and highly

reduced, anaerobic bacteria can use SO_4 as a terminal electron acceptor, the result being the production of H_2S (Reddy and DeLaune 2008). Sulfides are highly toxic to wetland plants (Koch and Mendelssohn 1989) and can limit nutrient uptake by inhibiting alcohol dehydrogenase (ADH) activity (Bradley and Morris 1990, Koch et al. 1990). Iron can reduce sulfide toxicity in the soil as a result of bacterial reduction of ferric iron before sulfate and through the precipitation of ferrous iron and sulfides (Gambrell 1994, Nyman et al. 1993a). ADH catalyzes the terminal step in alcohol fermentation, an anaerobic respiration process (Koch et al. 1990). If ADH activity is inhibited, less ATP may be produced, which can limit the ability of the plant to take in NH_4 (Koch et al. 1990).

Salinity exerts several stresses on plants, including osmotic, toxic ion, and nutrient stress. High salinities can cause plants to lose water through osmosis, which can dehydrate and kill plants less adapted to hypersaline conditions (Mahall and Park 1976). The salts in salt water are composed of ions that can be toxic to plants or can be transformed into ions that inhibit plant growth under certain conditions, such as sulfides (Kingsbury and Epstein 1986, Koch and Mendelssohn 1989). If salinities are high, K and other cation salts can compete with NH_4 at ammonium uptake sites, thus limiting NH_4 uptake (Smart and Barko 1980). Furthermore, some salt marsh species have been shown to require more N to support growth at higher salinities than lower salinities (Bradley and Morris 1992).

2.4.2 Decomposition

Decomposition is largely controlled by soil hydroperiod, which determines the type of respiration occurring and soil Eh. In the presence of oxygen, respiration occurs via aerobic respiration because O_2 is the most energy efficient electron acceptor (Nyman et al. 1993a). In the absence of oxygen, respiration occurs with less efficient electron acceptors, i.e. NO_3^-, Mn^{+4},

Fe^{+3}, SO_4^{2-}, and CO_2 (Nyman et al. 1993a). Eh measures electron pressure and indicates the intensity of reduction (Nyman et al. 1993a). Low Eh measurements (–300 to 400 mV) correspond to reduced conditions, and high Eh measurements (400 to 700 mV) correspond to oxidized conditions (Nyman et al. 1993a). As Eh decreases, less efficient electron acceptors are used, and the release of free energy decreases, as shown in the following equations:

$C_6H_{12}O_6 + 6O_2 \rightarrow 6CO_2 + 6H_2O = –2{,}877.4$ kJ mole^{-1} glucose

$5C_6H_{12}O_6 + 24NO_3^- + 24H^+ \rightarrow 30CO_2 + 12N_2 + 42H_2O = –2{,}720.92$ kJ mole^{-1} glucose

$C_6H_{12}O_6 + 12MnO_2 + 24H^+ \rightarrow 6CO_2 + 12Mn^{2+} + 18H_2O = –2{,}025.4$ kJ mole^{-1} glucose

$C_6H_{12}O_6 + 24Fe(OH)_3 + 48H^+ \rightarrow 6CO_2 + 24Fe^{2+} + 66H_2O = –1{,}591$ kJ mole^{-1} glucose

$C_6H_{12}O_6 + 3SO_4^{2-} + 6H^+ \rightarrow 6CO_2 + 3H_2S + 6H_2O = –482.2$ kJ mole^{-1} glucose

$C_6H_{12}O_6 \rightarrow 3CO_2 + 3CH_4 = –419.5$ kJ mole^{-1} glucose

The fact that Eh is higher in drained soils than flooded soils has an impact on the process of decomposition and plant productivity (Howes et al. 1986, Nyman and DeLaune 1991). Aerobic respiration rates are generally higher than anaerobic respiration rates (Nyman and DeLaune 1991). Decomposition of organic matter differs among marsh types; Nyman and DeLaune (1991) reported faster decomposition rates in fresh marshes than brackish and salt marshes. Other factors controlling decomposition in marshes include vegetation type, temperature, soil and plant fertility, and pH. Species with increased lignin content and more stems decompose relatively slowly (McKee and Seneca 1982, Melillo et al. 1982, Wilson et al. 1986). Warm temperatures and increased N content in soil and litter increase decomposition and microbial activity (Marinucci et al. 1983, Valiela et al. 1983, White and Trapani 1982). Soils with overly acidic or alkaline pH can result in lower decomposition rates (DeLaune et al. 1981b).

2.5 Determination of Accretion Rates

Several methods can be used to determine recent accretion rates (<150 years) in wetland systems. Some of these methods involve the use of radioisotope analysis of soil depth increments from a soil core, clay markers on the soil surface, or the depth of a specific characteristic in the soil profile that corresponds to a known event at or near the sampling site. Any of these methods can be applied given an appropriate set of environmental conditions.

2.5.1 ^{210}Pb Dating

A common method to determine ages of soil from a soil core involves using the decay rate of unsupported ^{210}Pb and the measured concentrations of the naturally occurring isotopes ^{210}Pb and ^{226}Ra at different depths of a soil core. ^{210}Pb is in the ^{238}U decay series and occurs through the decay of ^{226}Ra (half life 1622 years) to form the gas ^{222}Rn (half life 3.8 days), which decays through several short-lived isotopes to form ^{210}Pb (Robbins 1978). As ^{226}Ra decays in the soil, some ^{222}Rn may diffuse through the soil into the atmosphere, where it resides until it decays to ^{210}Pb (Robbins 1978). The unsupported ^{210}Pb is the component of total ^{210}Pb that is removed from the atmosphere by wet fallout or dry deposition, whereas the supported ^{210}Pb is derived from the *in situ* decay of eroded ^{226}Ra particles, i.e. the decay of ^{222}Rn that does not diffuse into the atmosphere (Oldfield and Appleby 1984). The supported ^{210}Pb is assumed to be in equilibrium with ^{226}Ra in the soil (Oldfield and Appleby 1984). The unsupported ^{210}Pb is the source that decays exponentially through time and is determined by calculating the difference between the measured total ^{210}Pb and supported ^{210}Pb in each soil increment. Using unsupported ^{210}Pb to determine accretion rates is very effective because nearly all unsupported ^{210}Pb becomes immobile in salt marshes once it reaches the soil surface (Benninger et al. 1975). However, physical or biological mixing can redistribute the soil-bound radioisotopes within the soil profile

or to other locations in the marsh (Robbins and Edgington 1975). The half-life of ^{210}Pb (22.26 yrs) limits a researcher's ability to date soils to within the last 100 to 200 years (Oldfield and Appleby 1984).

Total ^{210}Pb concentrations can be determined by a variety of methods. Some of these methods include measuring a sample's gamma-ray emissions (47 keV) with the use of a germanium detector (Bao et al. 2011, Liu et al. 2010), alpha spectrometry after dissolution in HNO_3, HCl, $HClO_4$, and HF (Craft and Richardson 1993, 1998), or through the measurement of ^{210}Pb daughter's (^{210}Bi) beta emission (Rama and Goldberg 1961). The gamma counting method is only applicable if large quantities of soil are available to be analyzed because the 47 keV emission of ^{210}Pb is only present in 4% of its disintegrations (Eakins 1982). The alpha and beta spectrometry methods can be effectively used on smaller amounts of soil. ^{226}Ra can also be measured in many ways, including measuring its gamma-ray emissions (295 keV) (Bao et al. 2011), the radon emanation technique (Sedlacek et al. 1980), or alpha counting a solid source (Koide and Bruland 1975).

The accretion rate can be determined by applying a model to the unsupported ^{210}Pb values. Three models commonly used to determine soil ages and/or mean accretion rates along a soil profile are the constant flux-constant sedimentation rate model (c.f.:c.s.) (Robbins 1978); the constant rate of supply (c.r.s.) model (Appleby and Oldfield 1978); and the constant initial concentration (c.i.c.) model (Appleby and Oldfield 1983). Each model has different assumptions that relate to different depositional conditions. The c.f.:c.s. model assumes a constant sedimentation rate and constant supply of unsupported ^{210}Pb through time, whereas the c.r.s. and c.i.c. models allow for varying sedimentation rates (Appleby and Oldfield 1983). The c.r.s. model assumes a constant fallout of unsupported ^{210}Pb to the soil surface over time, which results

in the dilution of unsupported ^{210}Pb as accretion rates increase (Appleby and Oldfield 1978). The c.i.c. model assumes that an increased flux of soil in the water column will remove a proportionally increased amount of unsupported ^{210}Pb from the water column (Appleby and Oldfield 1983). If the assumptions for the c.i.c. model are satisfied, sediments in the soil profile will all have the same initial concentration of unsupported ^{210}Pb and the associated radioactivity will decrease based on the exponential decay rate of ^{210}Pb (Appleby and Oldfield 1983). It should be noted that sedimentation rate as used in Robbins (1978), Appleby and Oldfield (1978), and Appleby and Oldfield (1983) has the same meaning as accretion used in this paper.

2.5.2 ^{137}Cs Dating

^{137}Cs is another isotope that can be used to determine recent average accretion rates (DeLaune et al. 1978). ^{137}Cs is artificially produced during nuclear fission, and its presence in the environment is attributed to atmospheric nuclear testing and releases from nuclear reactors (Ritchie and McHenry 1990). The depth with the highest ^{137}Cs concentration corresponds to the peak fallout of ^{137}Cs in 1963, and measurable activities first became present in 1954 (Pennington et al. 1973). Other smaller ^{137}Cs peaks may be identifiable in some soils that correspond to smaller fallout periods or regional events, such as the Chernobyl disaster (Callaway et al. 1998). The concentrations of ^{137}Cs can be measured without destruction of the sample by measuring its gamma-ray emission (662 keV) using a germanium detector (Ali et al. 2008, Campbell 1983). The average accretion rate since 1963 can be determined by dividing the depth of the ^{137}Cs peak by the difference in years between sample collection and 1963 (Nyman et al. 2006). ^{137}Cs preferentially adsorbs to fine soil particles such as clays and silts; however it is still adsorbed in lower concentrations by sands (He and Walling 1996). Some minerals bind more tightly with ^{137}Cs than others; ^{137}Cs adsorption on illitic clays is nearly irreversible (Lomenick and Tamura

1965), whereas montmorillonite and vermiculite clays form weaker bonds (Coleman et al. 1963, Staunton and Roubaud 1997). Similar to other radioisotopes, soil-bound ^{137}Cs can also become redistributed by biological or physical mixing processes, but the depths of peak horizons are not usually affected (Ritchie and McHenry 1990, Robbins and Edgington 1975).

2.5.3 Other Dating Methods

Similar to the ^{137}Cs dating method, ages of soils can be determined based on other known events unique to specific regions. Accretion rates estimated from large sand deposits using known dates of hurricane events in soil profiles have been closely related to measured accretion rates using the ^{137}Cs and ^{210}Pb methods (Turner et al. 2007). Very recent accretion rates ($\leq$1 year) can be determined by the feldspar clay marker technique as described by Cahoon and Turner (1989).

2.6 Liaohe River Delta

The Liaohe Delta is located in Liaoning Province, northeast China and adjacent to northern Liaodong Bay of the Bohai Sea (Figure 2.3). It is now supported by two separate rivers: the Shuangtaizi River and Daliao River. These two rivers became separated in 1958 when the old distributary that connected the two rivers was blocked south of the city Liujianfang. In 1968 the Panshan Sluice was built in the upper reaches of the Shuangtaizi River and has been in operation since that time. Similar to many other rivers in Northern China, the Liaohe River system is heavily polluted with metals and organic pollutants (Jusi 1989). Evidence of this pollution is well documented in Liaodong Bay and the Liaohe River system (Fu et al. 2011, Guo et al. 2007, Wan et al. 2008, Xu et al. 2009). Oil extraction is common throughout this region and has been in operation for at least 20 years. This region has a semi-humid temperate monsoon climate with an annual average precipitation of 612 mm (Li et al. 2010).

The Shuangtaizi River has a watershed area of 57,104 km^2 with a discharge and sediment load of about 4.3 x 10^9 m^3 yr^{-1} and 20 x 10^6 tons yr^{-1}, respectively (Zhang and Liu 2002). The Daliao River has a larger watershed area and discharge, but lower sediment load. It discharges about 8.7 x 10^9 m^3 yr^{-1} of water that carries about 18.5 x 10^6 tons yr^{-1} of sediment from its 164,104 km^2 watershed (Zhang and Liu 2002). Tidal ranges in the Liaohe Delta estuarine area are on average about 3.9 m, but can reach a maximum of 5 m during spring tides (Scott 1989, Yang and Chen 1995). Sediments are available to be deposited in the delta from tidal introduction of river and marine-derived sediment (Liu et al. 2008b).

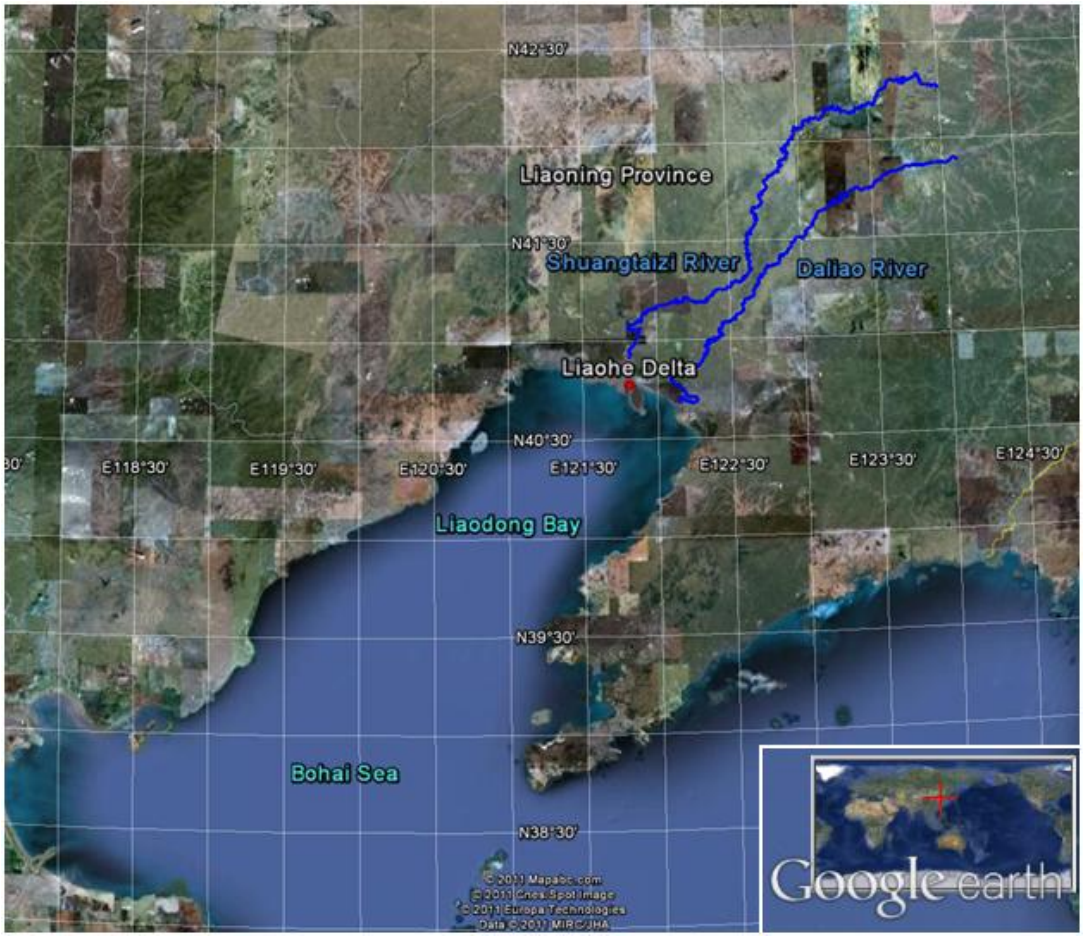

Figure 2.2: Liaohe Delta in Northeastern China.

The total area of fresh and salt marshes in the Liaohe Delta region is approximately 144,000 ha, excluding open water habitats (Liu et al. 2000). Various types of constructed and natural wetlands exist near the Liaohe Delta. The constructed, mostly freshwater wetlands are composed of cultivated rice paddies and farmed *P. australis* fields; the natural wetlands are composed of a variety of native fresh and salt marsh vegetation (Ji et al. 2009). The dominant salt marsh species in the Liaohe Delta, *Suaeda* spp., is designated different species names in the literature (e.g., *S. glauca, S. heteroptera, S. salsa*), but will be referred to hereafter as *Suaeda salsa*. *S. salsa* is a low-growing halophytic annual plant that can tolerate salinity and water table ranges from about 5 to 20 and –0.92 to 0.08 m, respectively (Baoshan et al. 2008). It is present in monotypic stands throughout the high intertidal zone of the Liaohe Delta.

3. MATERIALS AND METHODS

3.1 Sampling Locations

Soil cores were taken at nine sites within two areas in the intertidal zone of the Liaohe Delta, Liaoning Province, Peoples Republic of China: areas THZZH and SKZH (Figure 3.1). Only one core was taken at each site because replicate cores typically have the 1963 soil horizon in identical or adjacent layers (Nyman et al. 1993b, Nyman et al. 2006). The two areas were chosen based on their proximity to the mouth of the Shuangtaizi River, presence or lack of vegetation, and presence of clay material. Initially, the goal was to compare accretion rates in three different vegetation treatments of monotypic stands of *S. salsa*: mudflat, half cover, and full cover. Approximate vegetation density ranges for each vegetation treatment were determined by counting individual stems of *S. salsa* in a 1m by 1m quadrant in three locations at each sampling location. The average of the three counts was used to determine the minimum, median, and maximum stem counts for each vegetation treatment. It was assumed that vegetative cover of the sites remained constant over the time period that accretion rates were measured. Additionally, accretion rates were compared using the different elevations of the sites.

Three cores were taken from each vegetation treatment from both areas. Five total soil cores were taken from area THZZH: three from full cover, one from mudflat, and one from the half cover (Figure 3.2). Four total soil cores were taken from area SKZH: two from mudflat and two from the half cover (Figure 3.3). Area THZZH had a lower elevation and was closer to the mouth of the Shuangtaizi River than area SKZH. The sites within each area and treatment were chosen in locations that were representative of the surrounding salt marsh with respect to ostensibly similar vegetative cover and elevation. Cores were taken within the marsh in areas

that were undisturbed, at a distance of at least 50 m from all roads or levees and at least 10 m from all tidal channels. All cores were taken in areas that were not impounded by artificial or natural levees, i.e. high tides could inundate the marshes and deposit sediment in the sampling locations if tides reached high enough levels. Field measurements at each site included taking one soil core and measuring salinity, temperature, pH, Eh, and dissolved O_2 from pore water samples. Site locations were documented by their respective coordinates with a hand-held GPS unit.

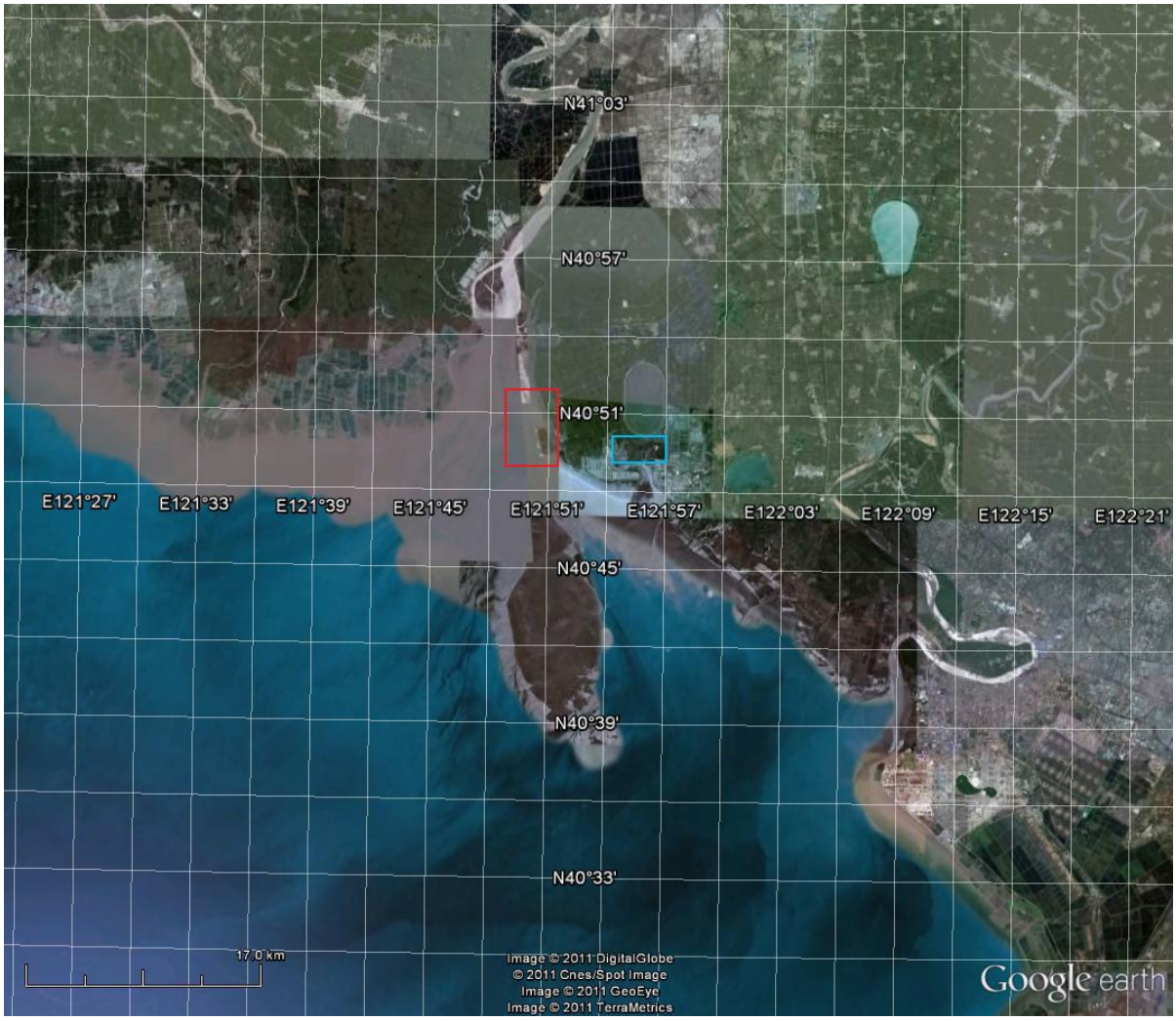

Figure 3.1: Sampling areas THZZH (red rectangle) and SKZH (blue rectangle).

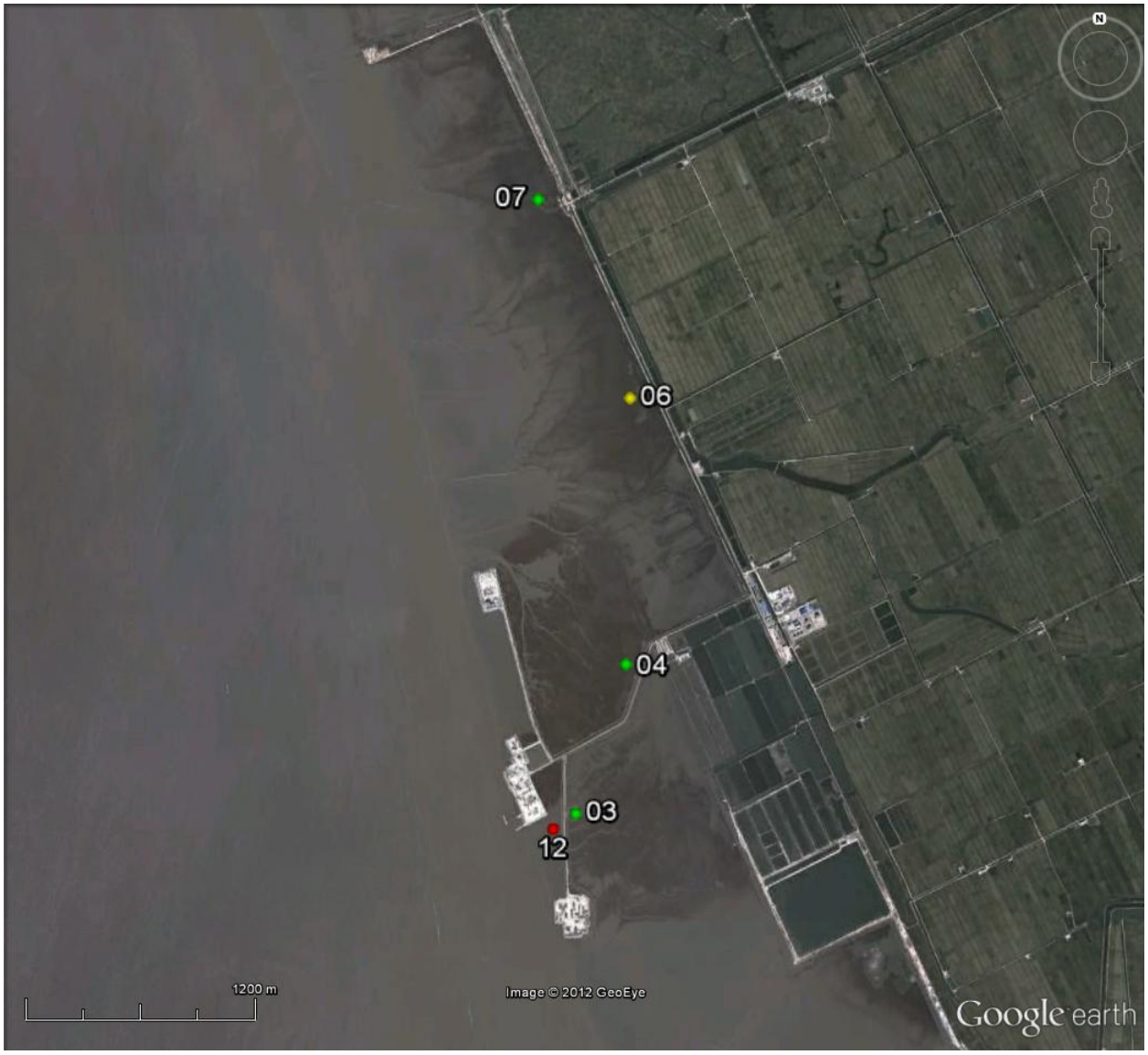

Figure 3.2: THZZH sampling sites. Three soil cores from full cover (green markers), one from half cover (yellow marker), and one from mudflat (red marker).

3.2 Sampling Methods

Soil cores were taken using a 15-cm diameter by 1-m long thin-walled metal cylinder with a machine sharpened end (Appendix I). This large diameter and thin-walled coring device was used to avoid compaction. The outside of the coring device was marked with 10-cm increments from the bottom of the cylinder so compaction could be measured within each 10-cm increment of soil. Compaction was determined by measuring the outside and inside of the metal

cylinder and subtracting the outside measurement from the inside measurement. The tube was slowly twisted into the soil until it reached a depth of 80 cm, or a depth at which compaction was approaching 10 cm. Soil cores ranged from 53.5 cm to 80 cm long. Once the appropriate depth was reached, a plug was placed in the top of the tube so that the surface soil would not be contaminated. The core was removed from the ground by digging around the core to the bottom of the cylinder, and then carefully covering the bottom with a clean circular piece of rubber while lifting the core out of the ground. Soil cores were sealed with temporary caps, transported horizontally in the cylinder to prevent further compaction, and placed in a freezer upon returning to the Wetlands Research Center. Elevation measurements were made in September 2011 at each location using a Leica, Total Station instrument. The mean sea level of the Yellow Sea was used as a reference elevation.

Before extruding the soil, the soil cores were allowed to thaw for several hours. A long, 5-cm diameter stick with a 14-cm diameter piece of wood nailed to one end was used to push the soil out of the tube. After extrusion, each core was measured again to document any change in length of the core after transporting, freezing, and extruding it. Soil cores were sectioned into 2.5-cm increments from the surface layer of soil down to the bottom of the core with a thin metal wire. Occasionally a serrated knife was used to cut through larger roots. Great efforts were made to ensure that the height of each increment was 2.5 cm by marking the increments on three sides along the entire length of the core before sectioning it and by carefully lining up the markings with the wire. In three cores, the bottom increments of soil were less than 2.5 cm due to compaction while extruding the cores, soil expansion during transportation or freezing, or the inability to reach a depth divisible by 2.5 due to compaction while taking the cores. Two cores had no compaction after extrusion: THZZH-03 and THZZH-04.

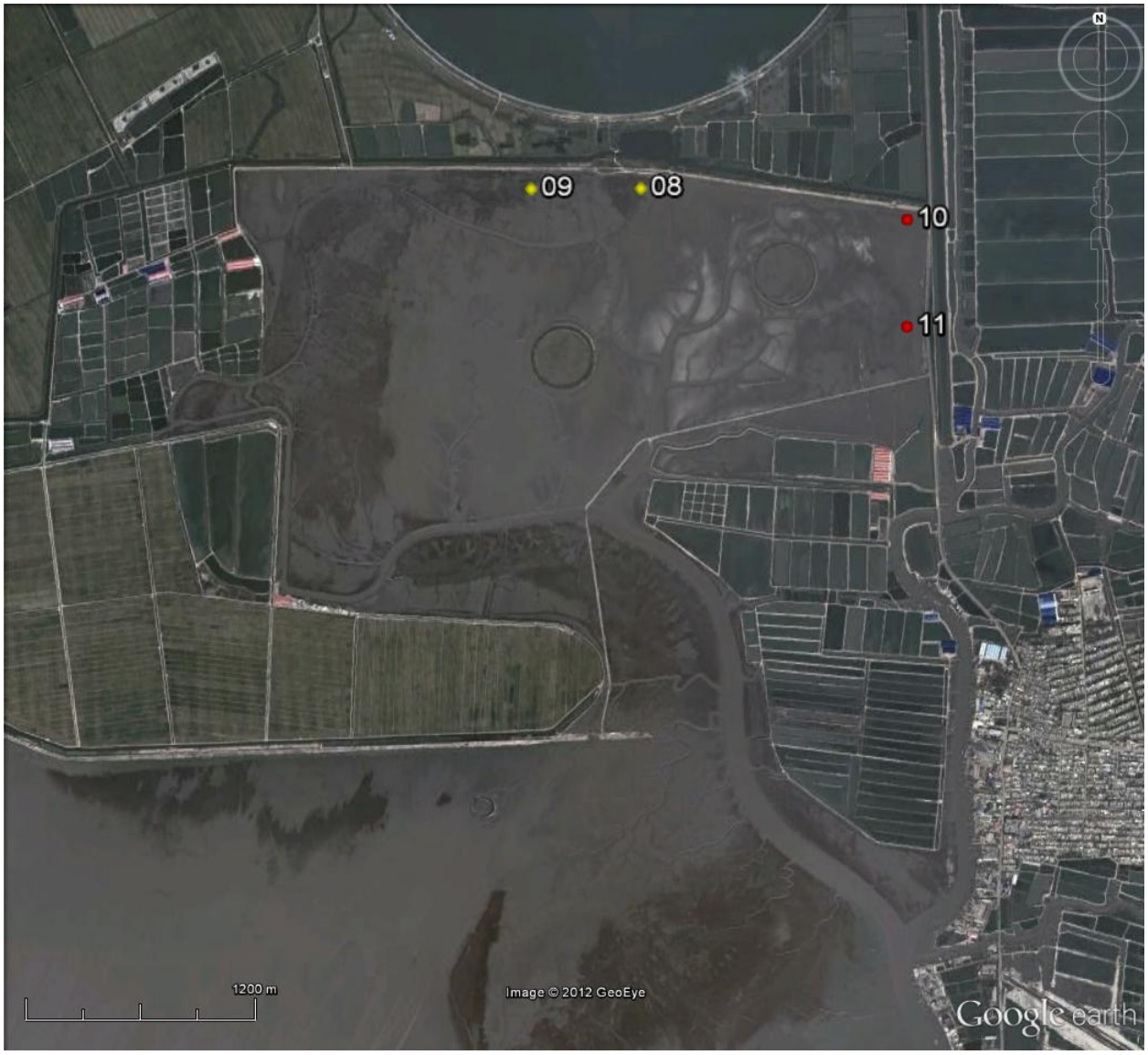

Figure 3.3: SKZH sampling sites. Two cores from half cover (yellow markers) and two cores from mudflat (red markers).

Pore water samples were taken within the marsh, adjacent to where each soil core was taken. A 20–30-cm hole was dug in the marsh and allowed to fill with soil pore water. A sample of this water was taken from each site and transported outside the marsh, where it was measured for salinity, temperature, pH, Eh, and dissolved O_2. pH and temperature measurements were taken using a portable pH meter (Jenco ltd., model 6010). Eh measurements were taken using the same meter, but with three Pt electrodes and a saturated calomel reference electrode. Salinity

and dissolved O_2 were measured with a portable salinity meter (Jenco ltd., model 3010) and a portable dissolved O_2 meter (Jenco ltd., model 9010), respectively.

3.3 Laboratory Measurements and Materials

Laboratory measurements were conducted at the Wetlands Research Center in Panjin, Liaoning Province and Qingdao Institute of Marine Geology (QIMG) in Qingdao, Shandong Province. For this project, laboratory measurements were carried out for bulk density (BD), grain size, inorganic matter (IM), mineral analysis, moisture content, organic matter (OM), organic carbon (OC), pH, radioisotope spectrometry, and sensitive grain size. Laboratory measurements occurred from June through December 2011. A full list of instruments and instrument precisions used for laboratory measurements can be found in appendix II.

3.3.1 Bulk Density and Moisture Content

The increments of soil were placed in pre-weighed cotton bags and weighed wet. Immediately after weighing the wet sample, approximately a 30-g or 60-g subsample of soil was taken from each increment of soil, placed in a pre-weighed aluminum foil pouch, weighed wet, and oven dried at 105 ^{o}C for 24 hours (Heng ke J, model DHG-9203A). After 24 hours, the masses of 2 to 3 samples were weighed and reweighed after an hour to ensure mass stabilization. The moisture content and remaining dry mass were applied to the entire increment to find percent moisture, percent dry mass, and BD of each soil increment. The percent moisture and percent dry mass for each subsample were assumed to be representative of the entire sample increment. The volume of each sample was calculated from the estimated height and radius of each increment of soil. In the cores where compaction occurred, the amount of compaction was divided equally among each increment of soil because the length of many cores changed after the initial measurement of compaction was documented while taking the cores.

3.3.2 Radioisotope Spectrometry

Soil samples were air-dried for at least one week and transported to QIMG for analysis. Approximately 300 g of each increment of soil were ground with a mortar and pestle, then oven-dried in beakers overnight at 105 ^{o}C (SANFA, model DHG-9202-2SA). Plastic 200 cm^3 cylindrical containers were oven dried at 65 ^{o}C for one hour and weighed. The oven-dried soil samples were placed in the dry 200 cm^3 containers and weighed to find the mass of oven-dried soil in each container (Mettler Toledo, model PL3001-S). Each container was capped and sealed with tape for at least 15 days to allow for ^{222}Rn to come into equilibrium with ^{226}Ra. Samples were counted for 25,200 seconds to find concentrations of total ^{210}Pb, ^{226}Ra, and ^{137}Cs by using a broad energy germanium detector (Canberra, model BEGe3830) with a low background noise lead chamber (Canberra, model 777A). Standard reference samples were used to determine counting efficiency and make volume corrections for ^{137}Cs (National Institute of Meteorology, P.R. China, Sample ZFCSE100316), ^{210}Pb, and ^{226}Ra (International Atomic Energy Agency, Sample IAEA-434). Furthermore, background ^{137}Cs, ^{210}Pb, and ^{226}Ra values were measured and subtracted from all results. Only samples from every other increment of soil were counted because of time constraints.

3.3.3 Organic Matter and Organic Carbon Analyses

OM determinations for each increment of soil were carried out in a manner similar to protocol described by Craft et al. (1991). Briefly, approximately 7–15 g of ground, air-dried samples were placed in quartz beakers and dried overnight in an oven at 105 ^{o}C. The samples were weighed to find the oven dry weight, then placed in a combustion chamber for 8 hours at 450 ^{o}C. The samples were taken out of the combustion chamber and placed back in the oven at 105 ^{o}C for 4–6 hours. This was done to ensure that after combustion no moisture would be

included in the mass of the sample that may have been gained while transporting the beakers. Percent OM was determined to be the percent mass that was lost during ignition. OC was inferred from OM as described by Craft et al. (1991) for use in estuarine systems with equation 1:

$$O_c = (0.40 \bullet LOI) + (0.0025 \bullet LOI^2) \quad (1)$$

where O_c = organic carbon (g) and LOI = mass lost during ignition (g). Duplicates were completed on fourteen samples for OM determination to ensure consistency within the same increment of soil.

3.3.4 Grain Size, Sensitive Grain Size, Clay Mineral Analysis, and pH

Grain size and sensitive grain size analyses were completed using a laser particle size analyzer (Malvern, Mastersizer 2000). A subsample of each increment of soil was collected and placed in individual beakers. The samples were dispersed and oxidized through addition of 20 mL of 15% H_2O_2 solution. After four hours, 5 mL of 0.5 normality $(NaPO_3)_6$ solution was added and allowed to fully disperse in the soil for at least two days. The dispersed samples were poured into individual containers and analyzed for grain size by the automated Mastersizer 2000. Sample grain sizes were separated into the USDA and ISSS soil texture categories sand, silt, and clay. Sensitive grain size analysis was completed in the same manner, but the soil was separated into 0.25Φ-size increments. Mineral analysis was completed only on core THZZH-03 to determine mineral type in the soil profile using an X-ray diffractometer (D/Max-2500). pH was determined by vigorously mixing a 2:1 ratio of de-ionized water and soil in small test tubes. pH was measured in each sample after allowing the solution in the sealed test tubes to sit for seven days (Mettler Toledo, model Seven Multi pH).

3.4 Accretion and Accumulation Rate Determination

The accretion rates and ages of increments throughout the soil profiles were calculated using the c.f.:c.s. model and c.r.s. model. If the c.f.:c.s. model assumptions are satisfied, then the unsupported ^{210}Pb concentrations vary according to equation 2:

$$A_x = A_s \bullet e^{-k \bullet d/s} \quad (2)$$

where A_x = the ^{210}Pb concentration at depth x, A_s = the ^{210}Pb concentration at the soil surface, k = the ^{210}Pb decay rate constant (0.03114 yr^{-1}), d = depth (cm), and s = soil accretion rate (Oldfield and Appleby 1984). If unsupported ^{210}Pb is plotted on a logarithmic scale against depth, the ^{210}Pb profile will be linear with the slope of the regression (m) = –k/s, and accretion rate = –k/m.

If the c.r.s. model assumptions are satisfied, then the unsupported ^{210}Pb concentrations vary according to equation 3:

$$A_d = A_o \bullet e^{-k \bullet t} \quad (3)$$

where A_d = the residual inventory of unsupported ^{210}Pb below depth d, A_o = the total inventory of unsupported ^{210}Pb, and t = the soil age in years (Appleby and Oldfield 1978). A_d and A_o are calculated by direct numerical integration of the unsupported ^{210}Pb profile (Appleby and Oldfield 1978). In order for this model to be applied, the least squares regression equation from the c.f.:c.s. model was used to estimate the remaining inventory of unsupported ^{210}Pb below the bottom soil increment because background unsupported ^{210}Pb values were not reached in any soil core. The age of each soil layer was calculated with equation 4.

$$t = (1/k) \bullet \ln(A_o/A_d) \quad (4)$$

Accretion rate (cm yr^{-1}) for the c.r.s. model was calculated by dividing the depth (cm) of an increment by the calculated age of the increment. All accretion rates were calculated using both

mass based activities (Bq kg^{-1}) and volume based activities (Bq 200 cm^{-3} container) to determine if BD had an effect on accretion and accumulation. Volume-based activities were based on 200 cm^{-3} and not the volumes of each soil increment because adjusting increment height for compaction caused differences in volumes among sample core increments.

Accumulation rates (g m^{-2} yr^{-1}) were calculated from the surface increment to the bottom increment as described by Nyman et al. (2006) with equation 5:

$$(\sum_{\text{increment with known age}}^{\text{surface}} bd \bullet h \bullet 10{,}000\ cm^2\ m^{-2})/t \quad (5)$$

where bd = the bulk density of the soil layer (g cm^{-3}), h = the height of the soil layer (cm), and t = age of soil increment. IM, OM, and OC accumulation rates were determined by using the same equation, but multiplying the BD of each increment by the percent inorganic, OM, or OC corresponding to that soil increment, respectively. Mean depths for each increment were used for equations 2–5. For the purposes of comparative analysis of accumulation within the same timeframe among cores, the depth corresponding to a common age was calculated with equation 6:

$$d = yr \bullet (-k/m) \quad (6)$$

This allowed bulk accumulation to be summed to depths corresponding to a common age among all cores.

3.5 Statistical Analysis

Descriptive statistics were used to characterize BD, OM, OC, mineral content, grain size, mineral composition, accretion rates, and accumulation rates in all soil cores. Standard errors (SE) were calculated at 95% confidence limits. Model 1 least squares regression analysis was used to calculate ^{210}Pb accretion rates in the c.f.:c.s. model because control was maintained over the independent variable (depth). Pearson's product-moment correlation coefficient was used for

three purposes: 1) to determine whether the regression model used to calculate accretion rates fit the data well enough to be applied, 2) to determine whether a correlation existed among the independent variable elevation and dependent variables accretion and accumulation rates, and 3) to determine the relationship among sources of accumulation (i.e., inorganic accumulation, organic accumulation) and accretion. A one-way analysis of variance (ANOVA) was used for hypothesis testing to determine whether a difference existed between sample means of accretion rates among vegetation density treatments and OC accumulation rates among vegetation density treatments. An analysis of covariance (ANCOVA) was applied to test whether accretion varied among vegetation density treatments while holding elevation constant. Regression analysis was also used to determine whether a relationship existed between elevation and accretion/OC accumulation. These statistical procedures are explained in detail in Sokal and Rohlf (1995). Statistical analyses were carried out using MatLab and SPSS software.

4. RESULTS

4.1 Field and Laboratory Measurements

Salinity values were lower at all the THZZH sites relative to the SKZH sites, except for sites SKZH-11 and THZZH-12 (Table 4.1). pH ranged from 6.81 at THZZH-03 to 8.36 at THZZH-12. The elevations of SKZH sampling sites were on average over 1.8 m higher than THZZH sampling sites. Eh and dissolved O_2 measurements were not included in the results because of errors during sample collection. It is likely Eh and dissolved O_2 content increased during the process of transporting the porewater samples to be measured.

Table 4.1: Vegetation, elevation, salinity, and pH measurements taken at each sampling location. *approximate vegetation density ranges: mudflat = 0 plants m^{-2}, half cover = 100–700 plants m^{-2}, full cover = 2,400–9,800 plants m^{-2}.

Site	Vegetation*	Elevation (m)	Salinity	pH
THZZH-03	full cover	–0.59	21.8	6.81
THZZH-04	full cover	1.05	24.4	7.19
THZZH-06	half cover	1.50	23.5	7.53
THZZH-07	full cover	1.49	21.4	6.90
THZZH-12	mudflat	–1.37	27.3	8.36
SKZH-08	half cover	2.11	25.0	7.39
SKZH-09	half cover	2.15	27.5	7.39
SKZH-10	mudflat	2.36	27.9	7.46
SKZH-11	mudflat	2.27	18.2	7.66

BD for THZZH and SKZH samples ranged from 0.74 to 1.51 g cm^{-3} and 0.62 to 1.43 g cm^{-3} and averaged 1.22 ± 0.02 g cm^{-3} and 1.03 ± 0.03 g cm^{-3}, respectively (Table 4.2). BD in THZZH samples typically increased with depth, whereas BD values in SKZH were relatively constant throughout the soil profile (Figure 4.1). BD differed among individual cores ($p < 0.01$), but did not differ among cores from below and above sea level ($p = 0.70$). Percent OM was on average higher in SKZH samples than THZZH samples, averaging 3.6 ± 0.2% and 3.2 ± 0.1%, respectively (Table 4.2). Because OC was inferred from OM concentrations, fluctuations in OC

were closely related to OM fluctuations and were highest in the half-cover vegetation density (Figure 4.1). OC was different among individual cores and vegetation treatments ($p < 0.01$), but not different among sites below and above sea level ($p = 0.65$). Mineral content mirrored changes in OM. Complete data sheets for BD, OM, OC, and IM can be found in appendix III.

Table 4.2: Mean and standard deviation of BD, OM, inorganic content, and OC from each core with corresponding vegetation densities. Full cover (a), half cover (b), and mudflat (c).

Cores	BD (g cm^{-3})	OM (%)	Inorganic (%)	OC (%)
THZZH				
03_a	1.12 (0.15)	3.5 (0.7)	96.5 (0.7)	1.4 (0.3)
04_a	1.28 (0.20)	2.6 (0.8)	97.4 (0.8)	1.1 (0.3)
06_b	1.33 (0.12)	3.1 (0.4)	96.9 (0.4)	1.3 (0.2)
07_a	1.17 (0.09)	3.7 (1.6)	96.3 (1.6)	1.5 (0.6)
12_c	1.20 (0.09)	3.1 (0.5)	96.9 (0.5)	1.3 (0.2)
SKZH				
08_b	0.99 (0.07)	3.8 (0.2)	96.2 (0.2)	1.5 (0.2)
09_b	0.88 (0.12)	4.1 (0.6)	95.9 (0.6)	1.7 (0.3)
10_c	1.18 (0.11)	3.2 (0.3)	96.8 (0.3)	1.3 (0.1)
11_c	1.09 (0.14)	3.2 (0.4)	96.8 (0.4)	1.3 (0.2)

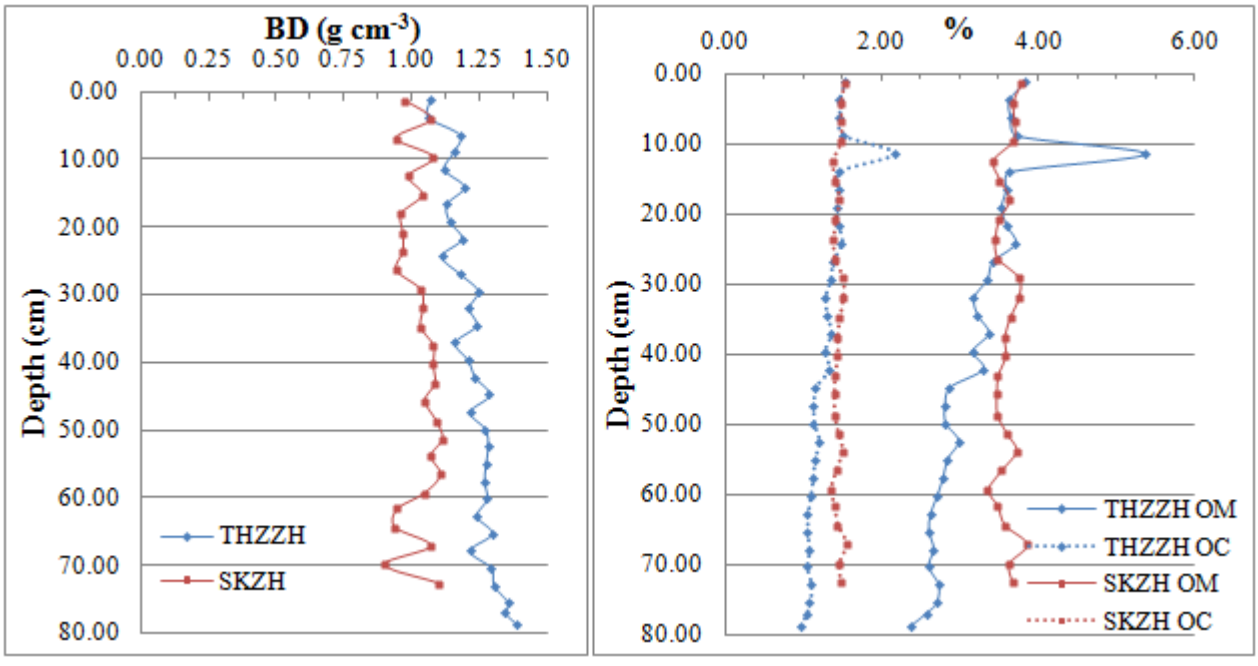

Figure 4.1: Mean BD, OM, and OC at different depths from areas THZZH and SKZH.

Soils from both areas were predominantly composed of silt-size particles with appreciable amounts of clay and sand (Figure 4.2). Mean percent sand, silt, and clay composition throughout THZZH were 9.8 ± 0.9%, 79.7 ± 0.8%, and 10.3 ± 0.2%; throughout SKZH these values were 5.8 ± 0.8%, 82.7 ± 0.6%, and 11.6 ± 0.3%, respectively. Sensitive grain size analysis did not result in any consistent discernable changes in grain size between depth increments. Mineral analysis from THZZH-03 showed a considerable illite content (≥ 44%) throughout the soil profile with a mean illite content of about 52%, and was highest near the surface sediment (59%) (Figure 4.3).

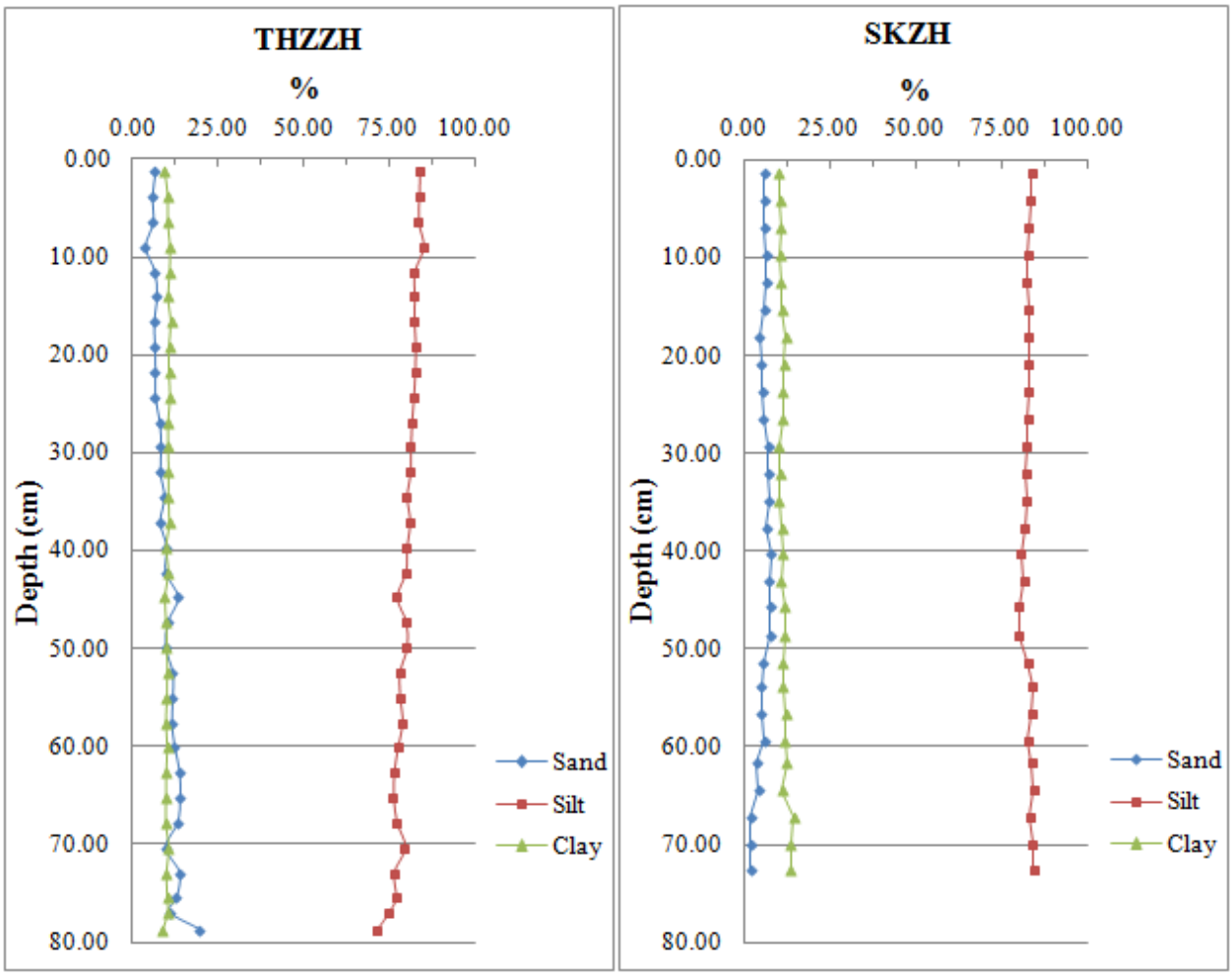

Figure 4.2: Mean grain size at different depths in areas THZZH and SKZH.

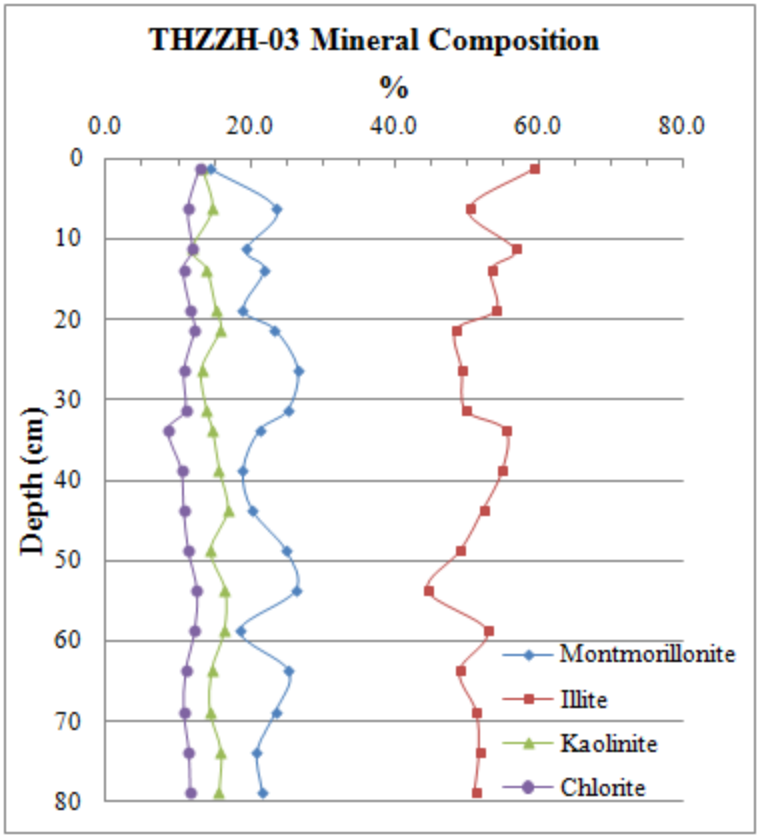

Figure 4.3: Mineral composition of THZZH-03

4.2 ^{137}Cs and ^{210}Pb Chronology, Accretion, and OC Accumulation

^{137}Cs values ranged from 1.33 to 7.96 Bq kg^{-1}, and profiles did not display any distinctive peaks that might have corresponded to the 1963 peak fallout of ^{137}Cs or reach background levels at depths that might have corresponded to layers preceding the initial detection of ^{137}Cs in 1954 (Figure 4.4). When mass-based ^{137}Cs activities were converted to volume-based activity, ^{137}Cs values became more compressed and displayed similar patterns to the mass-based activities. The small changes in grain size along soil profiles did not appear to have a major impact on ^{137}Cs activity. Because the 1963 peak horizon was not found in any core, it can be assumed that accretion rates at THZZH and SKZH sites were greater than 1.64 and 1.09 cm yr^{-1}, respectively.

Unsupported ^{210}Pb profiles were somewhat erratic, but overall displayed a decreasing trend with increasing depth (Figure 4.5). Accretion rates from both ^{210}Pb models using mass-

based activities ranged from 0.85 to 15.6 cm yr^{-1} (Table 4.3). When unsupported ^{210}Pb activities were converted to volume-based activities and applied to the models, accretion rates ranged from 0.89 to 21cm yr^{-1}. OC accumulation rates calculated using mass- and volume-based activities for both models ranged from 0.137 to 2.49 kg m^{-2} yr^{-1} and 0.144 to 3.15 kg m^{-2} yr^{-1}, respectively (Table 4.4). Some differences existed in the results obtained with different models and mass-based versus volume-based accretion rates; however, statistical testing using one-way ANOVA did not result in a significant difference of means among models for accretion based on mass activities (p = 0.63) or volume-based activities (p = 0.68). Similarly, there was no significant difference of means found among models for OC accumulation using mass-based accumulation rates (p = 0.72) or volume-based accumulation rates (p = 0.88).

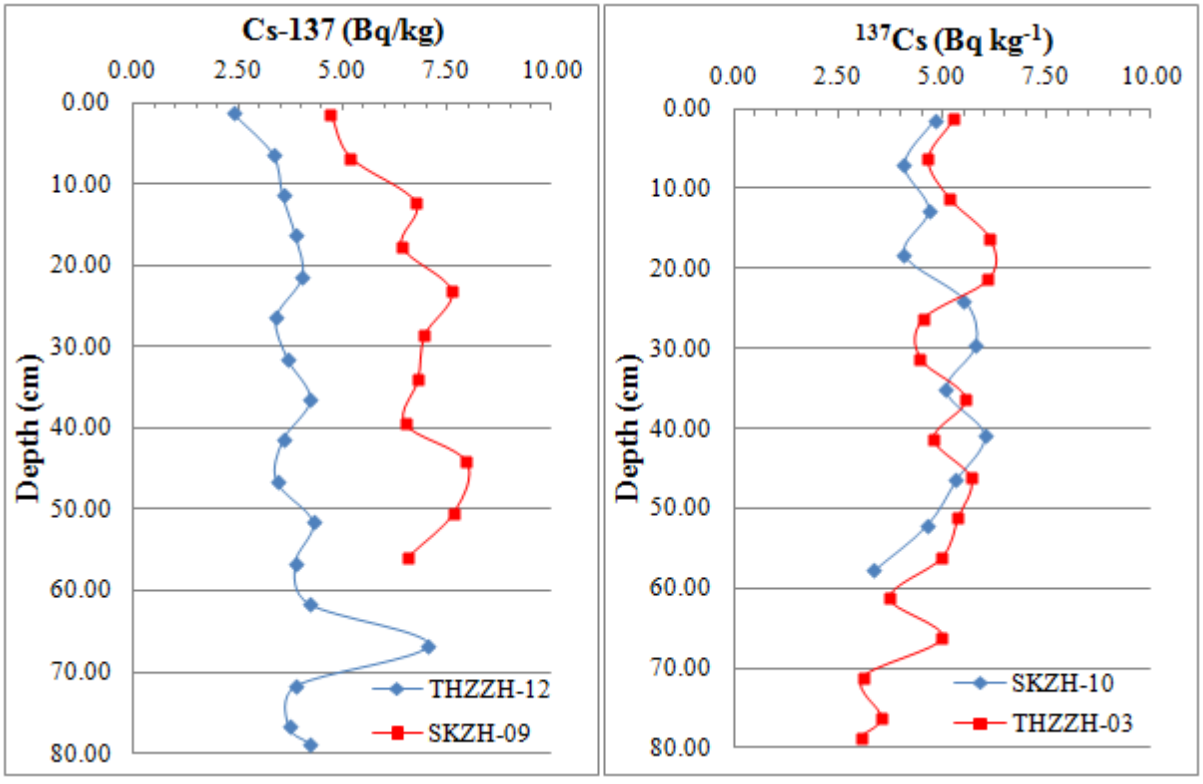

Figure 4.4: ^{137}Cs profiles from four sample cores.

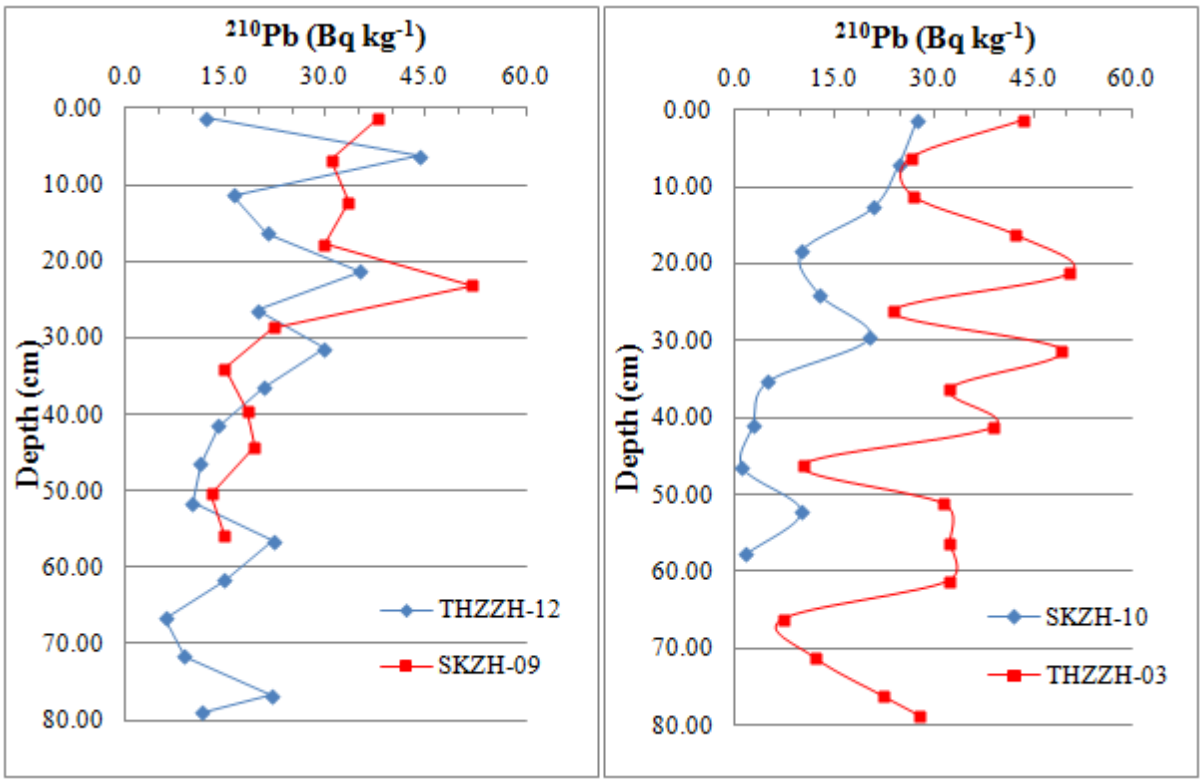

Figure 4.5: Unsupported ^{210}Pb profiles from four sample cores.

Table 4.3: Accretion rates calculated using mass activities (m) and volume activities (v) for each core with corresponding elevations and vegetation densities. Full cover (a), half cover (b), mudflat (c). *Correlation coefficients of the least squares regression equation used to calculate accretion were not significantly different from zero.

Site	Elevation	210Pb Accr Rt (cm yr^{-1})$_m$			210Pb Accr Rt (cm yr^{-1})$_v$		
	(m)	c.f:c.s.	c.r.s.	Mean	c.f:c.s.	c.r.s.	Mean
THZZH							
03$_a$	–0.59	6.77	5.23	6.00	9.73	7.91	8.82
04$_a$	1.05	2.68	1.66	2.17	3.35	2.21	2.78
06$_b$	1.47	1.56	0.87	1.21	1.67	0.94	1.31
07$_a$	1.49	10.38*	8.63*	9.51	11.12*	9.59*	10.35
12$_c$	–1.37	6.92	5.19	6.05	6.11	4.43	5.27
SKZH							
08$_b$	2.11	15.57*	14.58*	15.07	20.76*	19.10*	19.93
09$_b$	2.15	3.58	2.70	3.14	4.58	3.69	4.14
10$_c$	2.36	1.46	0.85	1.15	1.52	0.89	1.21
11$_c$	2.27	1.98	1.30	1.64	2.21	1.47	1.84

Table 4.4: OC accumulation rates calculated using mass activities (m) and volume activities (v) of ^{210}Pb for each core with corresponding elevations and vegetation densities. Full cover (a), half cover (b), mudflat (c). *Correlation coefficients of least squares regression equation used to calculate increment age were not significantly different from zero.

Site	Elevation	OC Accum Rt (kg m^{-2} yr^{-1})$_m$			OC Accum Rate (kg m^{-2} yr^{-1})$_v$		
	(m)	c.f.:c.s.	c.r.s.	Mean	c.f.:c.s.	c.r.s.	Mean
THZZH							
03$_a$	–0.59	1.06	0.817	0.938	1.52	1.24	1.38
04$_a$	1.05	0.351	0.217	0.284	0.438	0.290	0.364
06$_b$	1.47	0.259	0.144	0.201	0.278	0.155	0.217
07$_a$	1.49	1.82*	1.51*	1.67	1.95*	1.68*	1.82
12$_c$	–1.37	1.06	0.797	0.929	0.935	0.678	0.807
SKZH							
08$_b$	2.11	2.49*	2.21*	2.35	3.15*	2.90*	3.03
09$_b$	2.15	0.526	0.397	0.462	0.673	0.543	0.608
10$_c$	2.36	0.235	0.137	0.186	0.246	0.144	0.195
11$_c$	2.27	0.278	0.183	0.231	0.310	0.207	0.258

The primary hypotheses were tested using one-way ANOVA and regression analysis to determine differences among vegetation density treatments and the relationship between elevation and accretion, respectively. Accretion rates did not differ among vegetation density treatments ($p > 0.50$) when using mass- or volume-based activities applied to both models. However, accretion rates did differ between sites below and above sea level ($p < 0.02$) in all models using both mass and volume activities. OC accumulation rates did not differ among vegetation density treatments ($p > 0.47$), but all models did differ among sites below and above sea level ($p < 0.02$). ANCOVA analysis revealed no differences in slopes ($p > 0.13$) or intercepts ($p > 0.84$) among regressions of accretion versus elevation for the different vegetation density treatments, regardless of whether accretion was calculated using mass- or volume-based unsupported ^{210}Pb activities. Similarly, when ANCOVA was applied to OC accumulation rates while using the same independent variables, there were no significant differences among slopes ($p > 0.05$) or intercepts ($p > 0.84$). These results suggest that the relationship between accretion

and elevation is independent of the vegetation density of the sites. The relationship between elevation and accretion/OC accumulation becomes very clear when these parameters were plotted in a scatter diagram (Figure 4.6). Considerable negative correlation exists between site elevation and the two dependent variables, accretion (R = –0.83, p = 0.01) and OC accumulation (R = –0.83, p = 0.01). Calculated accretion rates from cores THZZH-07 and SKZH-08 were not used for hypothesis testing or correlation analysis because there was sufficient scatter in the unsupported ^{210}Pb values that correlation coefficients and regression coefficients were not significantly different from zero in these cores ($p > 0.05$).

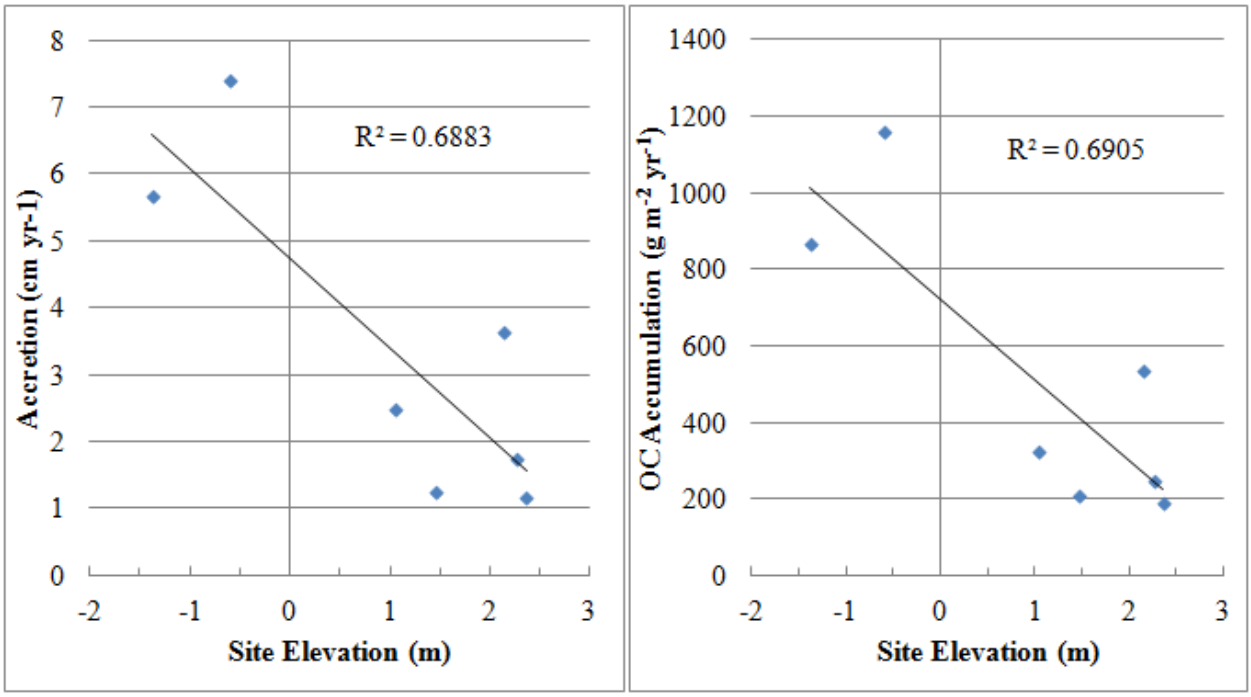

Figure 4.6: Mean accretion and OC accumulation from all models plotted against elevation.

OM accumulation was plotted against IM accumulation since 2001 to determine whether these parameters were independent of one another. A ten-year period was chosen because most sample soil cores were long enough to reach a soil depth corresponding to an age of ten years as calculated by the c.f.:c.s. model. Only the c.f.:c.s model was used because it assumes a constant accretion rate regardless of the time interval. This assumption allows one to calculate the depth

of an increment at a certain age using the same regression coefficient applied to the entire soil profile. Results from this analysis indicated OM and IM accumulation were highly correlated ($R > 0.97$). Thus these parameters were not independent of one another. Accretion was then plotted against accumulation (OM and IM), mean percent OM, and mean percent IM since 2001 to determine to what extent the variance of the accretion rates could be explained by differences in IM accumulation, OM accumulation, percent OM, or percent IM. If accretion and an independent variable were significantly correlated, then the differences in the corresponding independent variable may explain a significant percentage of the variance in accretion rates. Conversely, if accretion was uncorrelated with an independent variable, then the independent variable would not account for the observed variation of accretion rates.

Correlation analysis suggested that accretion was related to OM accumulation ($p < 0.001$) and IM accumulation ($p < 0.001$), but not related to percent OM or percent IM ($p > 0.06$), using mass-based activities. Similarly, using volume-based activities, correlation analysis indicated that accretion was related to OM accumulation ($p = 0.001$) and IM accumulation ($p = 0.002$), but not related to percent IM or OM ($p > 0.48$). Corresponding R^2 values were greater than 0.89 when accumulation was plotted with accretion (Figure 4.7) and less than 0.40 when percent OM/IM was plotted with accretion (Figure 4.8). These results indicate that roughly 89% of the variance in accretion is accounted for by differences in accumulation and that only a small percentage of the variance (if any) in accretion is accounted for by differences in percent IM or OM in the cores over the last ten years.

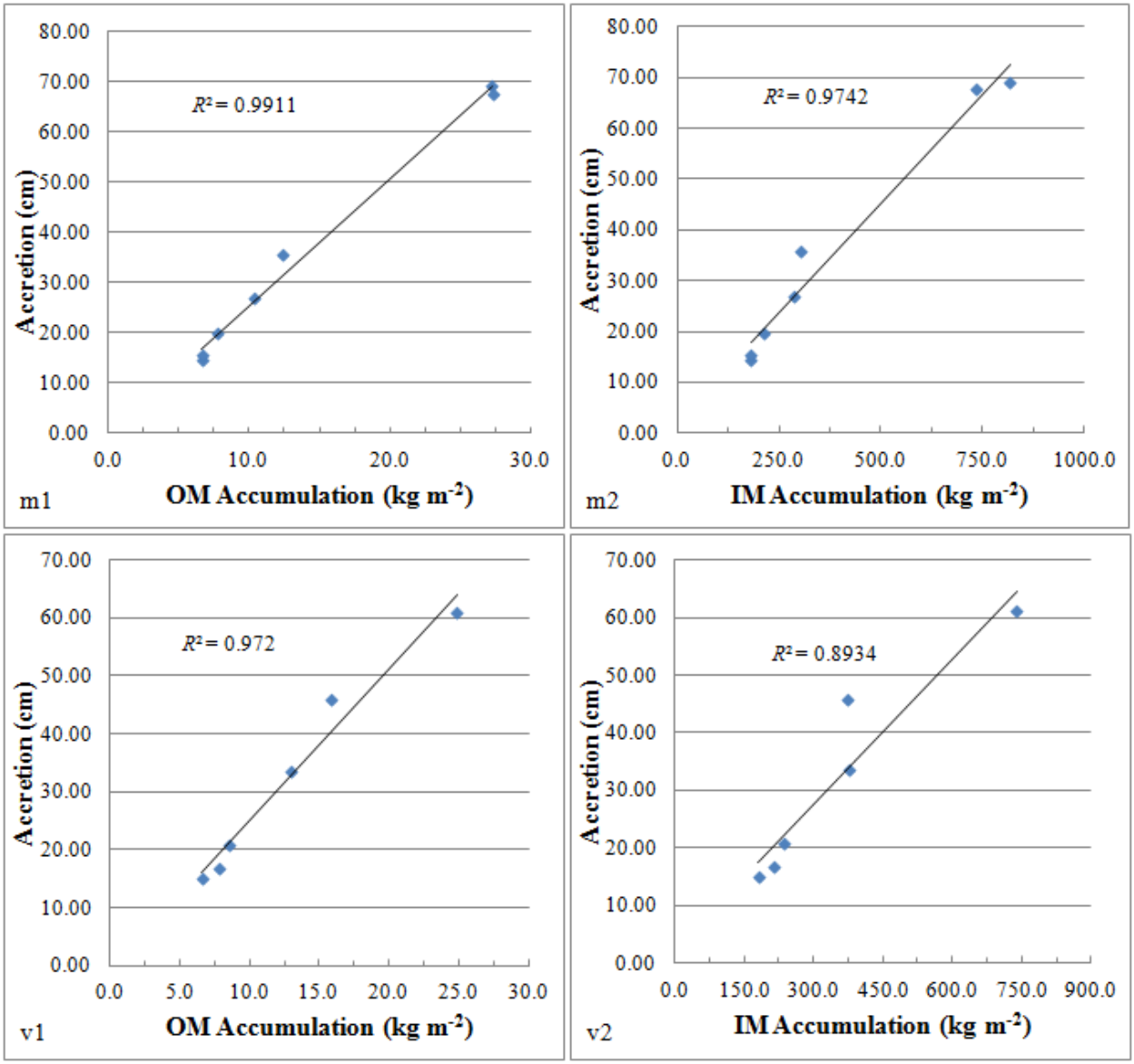

Figure 4.7: Relationship between accretion and accumulation using mass (m1, m2) and volume (v1,v2) ^{210}Pb activity since 2001. Cores 07 and 08 were excluded from all analyses.

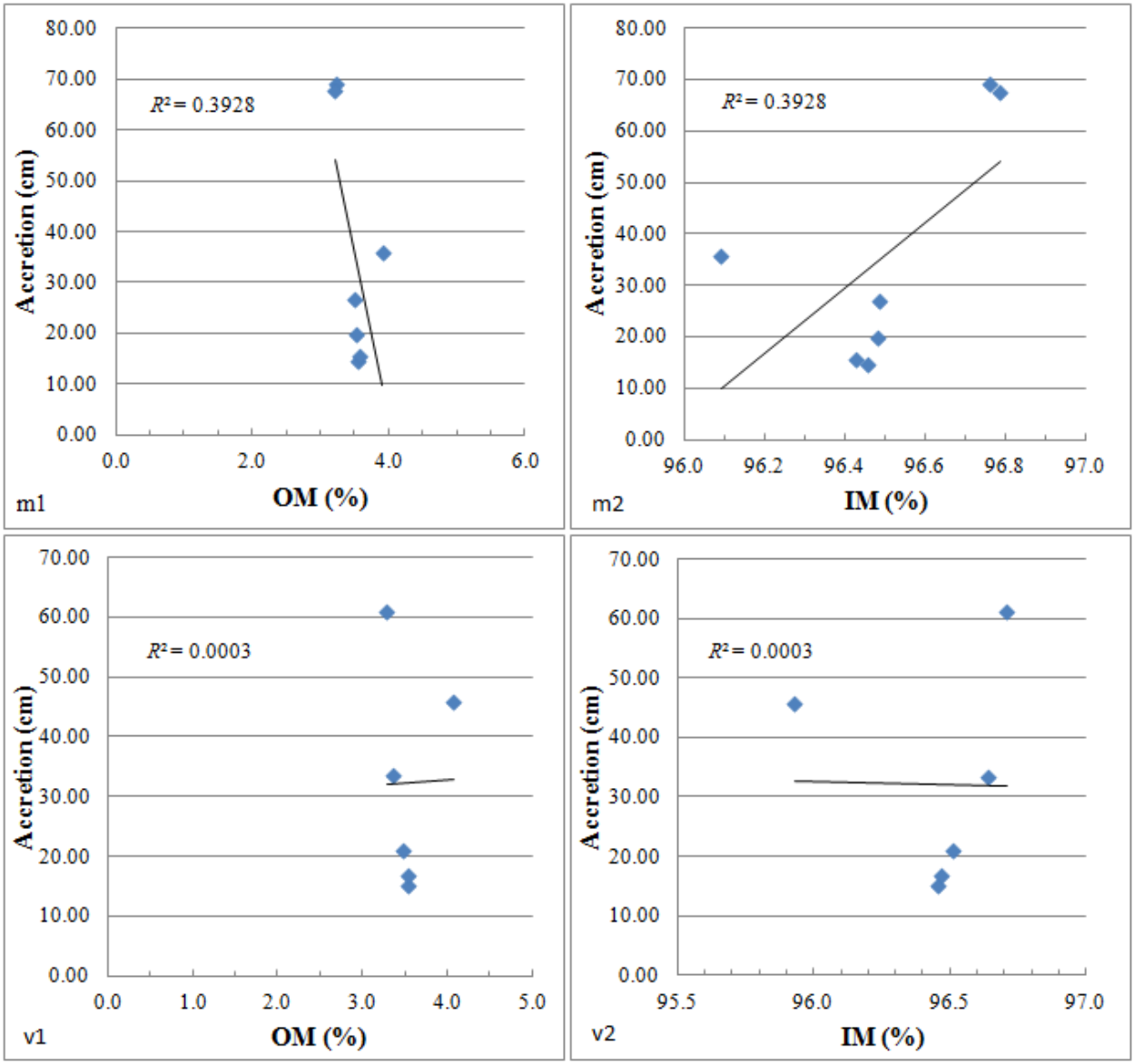

Figure 4.8: Relationship between accretion and percent OM and IM using mass (m1, m2) and volume (v1, v2) ^{210}Pb activity since 2001. Cores 07 and 08 were excluded from all analyses.

5. DISCUSSION

5.1 Influence of Models and Mass Versus Volume Based Activities

The ^{210}Pb models used to date soils have inherent differences that cause the age and accretion calculations to differ slightly among models. As previously described, the c.f.:c.s. model uses the trend (or slope) of unsupported ^{210}Pb activity along a depth profile, not the measured activities, to determine accretion rates (Oldfield and Appleby 1984). This would limit the effect of any abnormally high or low measured ^{210}Pb activities on the calculated accretion rate. The c.r.s. model, as applied to this research, uses the actual recorded values of unsupported ^{210}Pb at different depths and cumulative residual ^{210}Pb below the specified depth (estimated by direct numerical integration of the ^{210}Pb profile) to calculate the age of each increment (Appleby and Oldfield 1983). These differences in calculations caused the small differences in accretion rates and OC accumulation rates among models. Differences in accretion and OC accumulation among models were not significant, and did not change the conclusion that accretion and OC accumulation rates were different among sites above and below sea level.

Converting mass activities to volume activities required the application of BD to the mass activities (Bq kg^{-1}), which was previously unaccounted for during radioisotope spectrometry. Therefore, differences in accretion and OC accumulation among calculations using mass and volume activities resulted from the differences in BD. These differences in accretion and OC accumulation rates were not significant and did not change the conclusion that accretion and OC accumulation rates were different among sites above and below sea level.

5.2 Accuracy of Accretion and OC Accumulation Rates

Accretion and OC accumulation results from this paper should be viewed while considering the potential for error associated with the calculated rates. While the differences in

calculated rates between models using mass and volume activities were not significant, they were apparent. The fact that these models rest on assumptions that may or may not be entirely met by the conditions of sampling sites can introduce error into the calculations. Furthermore, the inability to locate the 1963 soil horizon in all cores limits the ability of the researcher to validate rates calculated using ^{210}Pb. Additional sources of error may include depositional conditions at sampling sites that allow for resuspension and focusing of soil or erosion and subsequent deposition of older sediment from the river watershed (Oldfield and Appleby 1984). Sediment resuspension may have caused low topsoil unsupported ^{210}Pb activity at some sites, whereas the focusing of the resuspended sediment may have caused elevated unsupported ^{210}Pb activities near the surface at other sites (Oldfield and Appleby 1984). Erratic ^{210}Pb profiles and high ^{137}Cs activities in near-surface sediments may suggest the potential for the deposition of older eroded sediment, which may explain the presence of lower and higher ^{210}Pb and ^{137}Cs activities in upper portions of soil profiles, respectively (Oldfield and Appleby 1984). All of these sources of error can potentially influence the unsupported ^{210}Pb activity along a soil profile, thereby changing the inputs to the ^{210}Pb models and accretion rates. This is why the range of accretion and OC accumulation rates among all models and activities is likely a more appropriate representation of accretion and accumulation processes within this system, as opposed to absolute accretion and OC accumulation rates.

5.3 Explanation of Accretion Results

Information on recent accretion rates in the Liaohe Delta region is limited to a single known publication discussing the sedimentary record of metals. Using ^{137}Cs radioisotope analysis of one core from tidal flats in the Shuangtaizi Estuary, Liu et al. (2011) reported mean accretion rates since 1954 to be 1.3 cm yr^{-1}. It should be noted that several differences exist

between the methods of Liu et al. (2011) and those applied in this paper; in the Liu et al. (2011) report, the sampling location was in a higher energy environment (i.e., within the mouth of the Shuangtaizi River), resolution of the ^{137}Cs profile was 6 cm, and small sample sizes were used for radioisotope spectrometry (6–10 g samples). Accretion rates from this research are within or exceed the range of accretion rates from other publications from coastal marshes in China, Louisiana, and Connecticut (Table 5.1).

Table 5.1: Accretion rates from coastal marshes from China, Louisiana, and Connecticut. *Accretion rates of THZZH-07 and SKZH-08 were not included.

Location	Vegetation Type	Method	Accretion (cm yr^{-1})	Source
Shuangtaizi Estuary, Liaoning, China	*Suaeda salsa*	^{137}Cs, ^{210}Pb	> 1.09, 0.85–9.73	This paper*
Shuangtaizi Estuary, Liaoning, China	*Suaeda heteroptera*	^{137}Cs	1.3	Liu et al., 2011
Wanggang, Jiangsu, China	*Suaeda salsa*, *Spartina* spp.	^{137}Cs, ^{210}Pb	3.08, 3–5.3	Wang et al., 2005
Xinyanggang, Jiangsu, China	*Suaeda salsa*, *Spartina* spp.	^{137}Cs, ^{210}Pb	1.9–4, 1.9–3.5	Liu et al., 2010
Coastal Louisiana, USA	*Spartina alterniflora, S. patens*	^{137}Cs	0.59–0.98	Nyman et al. 2006
Stonington, Connecticut, USA	*S. patens*	^{137}Cs, ^{210}Pb	0.17–0.40, 0.091–0.356	Orson et al. 1998

The inability to locate a peak ^{137}Cs activity at depth in all profiles can be best explained after analyzing these profiles in conjunction with corresponding ^{210}Pb accretion rates, grain size profiles, and mineral composition. In order to use ^{137}Cs to calculate accretion, several conditions must exist at the sampling sites: presence of mineral material that limits ^{137}Cs mobility (Lomenick and Tamura 1965), predominance of fine grain size particles (He and Walling 1996), and the ability to reach depths in a soil profile that correspond to specific events. Furthermore, it is favorable to have undisturbed depositional conditions at all sampling locations. Results from

mineral composition and grain size analysis indicated that the mobility of ^{137}Cs within the profile or adsorption of ^{137}Cs onto soil particles should not be an issue given the substantial presence of illites at site THZZH-03 (mean = 51.8%) and predominance of fine sediment particles (i.e., silt, clay) throughout the soil profiles (Figure 4.2). Depositional conditions at sampling sites were such that some physical mixing or bioturbation may have occurred, given the lack of vegetation at some sites and ubiquitous presence of crabs and other benthic macroinvertebrates. However, it is unlikely for these processes to cause the 1963 horizon to move to another layer (Ritchie and McHenry 1990, Robins and Edgington 1975). This evidence suggests that accretion rates are sufficiently high such that marker horizons corresponding to 1963 and 1954 were not reached. The majority of ^{210}Pb accretion rates calculated with both models using mass and volume activities support this hypothesis. All ages of bottom depth increments were calculated to be less than 48 years (Table 5.2) with the exception of 4. It should be emphasized that ages of bottom depth increments in the same cores (06 and 10) using the c.f.:c.s. model were less than 48 years.

Table 5.2: Calculated ages of soil core bottom depth increments using mass (m) and volume (v) based ^{210}Pb activities applied to both models. *Correlation coefficients of the least squares regression equation used to calculate accretion were not significantly different from zero.

Sample Core	Bottom Depth (cm)	Age (yr before 2011)m			Age (yr before 2011)v		
		c.f.:c.s.	c.r.s	Mean	c.f.:c.s.	c.r.s.	Mean
THZZH							
3	78.75	11.6	15.1	13.3	8.1	10.0	9.0
4	78.75	29.3	47.6	38.4	23.5	35.6	29.5
6	69.24	44.5	79.9	62.2	41.4	74.0	57.7
7	78.67	7.6*	9.1*	8.3	7.1*	8.2*	7.6
12	78.99	11.4	15.2	13.3	12.9	17.8	22.1
SKZH							
8	72.63	4.4*	5.0*	4.7	3.5*	3.8*	3.7
9	55.91	15.6	20.7	18.2	12.2	15.1	13.7
10	57.77	39.7	68.4	54.0	38.0	64.8	51.4
11	52.08	26.3	39.9	33.1	23.6	35.3	29.4

Accretion results from ^{210}Pb analysis suggest there is no significant difference among vegetation density treatments. Initially, assumptions were made that the vegetation density within each vegetation treatment had remained constant during the period accretion rates would be measured. However, aerial photography or other vegetation sampling reports were not available to substantiate this assumption. The composition of the vegetation at the sampling locations could have changed during the period of time associated with the calculated accretion rates, which may have affected accretion. It is also possible that vegetation does not have a major influence on accretion in this region. This has been reported in macrotidal low marsh areas where accretion is driven by IM accumulation (Temmerman et al. 2004).

Regression analysis revealed a significant negative correlation between elevation and accretion at the sampling sites. It seems logical that lower elevation sites would be flooded more frequently, which in turn would increase the period of time suspended sediment can be deposited. This theory is supported by significantly different accretion rates among sites below and above sea level. Higher accretion rates in lower elevation marshes have been previously reported in macrotidal salt marshes in the Bay of Fundy (Chmura et al. 2001) and microtidal salt marshes in Louisiana (Cahoon and Reed 1995). It is important to note that even though elevation and accretion were negatively correlated, lower elevation was not always associated with increased accretion at all sites. Furthermore, the fact that elevation was negatively correlated with accretion does not necessarily mean lower elevations caused greater accretion.

It is likely that a myriad of factors are causing high accretion rates in this region that were not all accounted for in this study. The extraction of oil throughout the Liaohe Delta region may be causing subsidence in addition to the natural subsidence occurring there (Morton et al. 2002, Xue et al. 2005). This could allow for accretion rates at least as high as the rate of the amplified

relative sea level rise, which could be reason for consistently high accretion rates through time. The total suspended sediment concentration of tidal water was not quantified in this study and may be very high relative to other marshes with similar hydrologic regimes. This could allow for increased suspended sediment deposition during each period of inundation.

5.4 Explanation of Accumulation Results

To my knowledge, there are no known published reports of OC accumulation rates within the Liaohe Delta. However, literature on OC accumulation within tidal salt marshes in other areas around the world is extensive. Chmura et al. (2003) provides a thorough review of soil carbon accumulation rates in salt marshes from various locations in the Gulf of Mexico, Atlantic, Mediterranean, and Northeast Pacific. All OC accumulation rates from this paper are within the range or exceed the range of those reported in Chmura et al. (2003) (Table 5.3). These results are comparable because OC accumulation rates were calculated using the same equation for organic carbon from Craft et al. (1991).

Table 5.3: OC accumulation rates in selected salt marshes around the world from this paper and Chmura et al. (2003). *OC accumulation from THZZH-07 and SKZH-08 were not included.

Location	Latitude	Vegetation Type	OC Accumulation ($g\ m^{-2}\ yr^{-1}$)	Original Source
Shuangtaizi Estuary, Liaoning Province, China	40°N	*Suaeda salsa*	137–1,522	This paper*
Scheldt, Netherlands	51.5°N	*Spartina anglica*	587–650	Oenema and DeLaune 1988
Long Island Sound, Connecticut, USA	41.2°N	*Spartina alterniflora*	72–204	Anisfeld et al. 1999
Rhone Delta, France	43.3°N	unavailable	161	Hensel et al. 1999

OC accumulation results suggest there is no significant difference in accumulation rates among vegetation density treatments. Similar to accretion, the lack of difference in OC

accumulation between vegetation density treatments may be due to changes in the composition of the vegetation at the sites through time or a limited effect of vegetation on OC accumulation. Differences did exist in OC accumulation rates among sites below and above sea level, and regression analysis indicated a significant negative correlation between OC accumulation and elevation. Higher OC accumulation rates at the below-sea-level sites was likely caused by increased accretion of soil with similar percent OC as that found in the above-sea-level sites. This theory is supported by the lack of difference in percent OC among sites below and above sea level and significantly greater accretion at the below sea level sites. This conclusion agrees with the results from Connor et al. (2001) that percent OC may not be a useful measure to predict OC accumulation potential in some salt marshes. Additionally, the higher accretion rates are reason for higher OC accumulation rates at sites below sea level because accumulation is to first approximation the product of accretion and concentration.

Results from correlation analysis of accumulation and accretion indicate that the variance in accumulation (OM or IM) accounts for the majority of the variance in accretion (> 89%), whereas variance in percent OM/IM accounts for minimal variance in accretion. Furthermore, mean percent OM/IM was very similar among all cores, ranging from 3 to 4%, irrespective of vegetation being present at sampling sites. The presence of OM throughout the soil profiles at unvegetated and vegetated sites may indicate that OM is consistently introduced via allochthonous particulate OM associated with allochthonous suspended sediments. Documentation of tidal introduction of particulate OM to salt marshes and estuarine systems around the world is well represented in the literature (e.g., Ogrinc et al. 2005, Wolff et al. 1979), as is evidence of considerable organic pollutants within the Liaohe River system (Guo et al. 2007, Jusi 1989). Collectively, this suggests that the sediment composition was very similar

among all sites, and the major factor causing differences in accretion was differences in accumulation among sites.

6. CONCLUSIONS

This was the first known study with the explicit purpose of determining accretion and OC accumulation rates in the Liaohe Delta. Results from ^{137}Cs and ^{210}Pb analyses indicated that most accretion rates were comparable to rates from other areas of China, but were very high relative to other reported accretion rates from coastal Louisiana and Connecticut. Accretion rates were estimated to be greater than 1.09 cm yr^{-1} in all cores based on ^{137}Cs techniques, from 0.85 to 9.73 cm yr^{-1} based on ^{210}Pb techniques, and were highest at sites THZZH-03 and THZZH-12 (excluding cores 07 and 08). The conclusion that accretion was too rapid to reach the 1963 horizon given the lengths of soil cores was supported by most calculated ^{210}Pb accretion rates, presence of illites, and predominance of fine grain size particles at sampling sites. The wide range in accretion rates using ^{210}Pb techniques was attributable to small differences among ^{210}Pb models using mass and volume based activities and a significant difference among sites that were below and above sea level. A lack of difference in accretion among vegetation treatments required the acceptance of the null hypothesis. This lack of difference may be attributable to changing vegetation density through time or limited influence of vegetation on accretion. Further analysis revealed a significant negative correlation between elevation and accretion, which suggests accretion is greater at lower elevation sites. This may be caused by increased hydroperiod of the soil surface and/or other parameters not measured, such as a high suspended sediment load in tidal waters. These same factors may be the reason for higher accretion in these marshes than in many salt marshes of North America.

Calculated OC accumulation rates from this research were within the range or exceeded the range of those reported in Chmura et al. (2003). OC accumulation rates ranged from 137 to 1,522 g m^{-2} yr^{-1} and were highest at sites THZZH-03 and THZZH-12 (excluding cores 07 and

08). Similar to accretion rates, the wide range in OC accumulation rates was attributable to small differences between ^{210}Pb models using mass and volume based activities and a significant difference between sites below and above sea level. Additionally, the lack of difference in percent OC between sites below and above sea level and significant difference in OC accumulation between those sites suggests percent OC may not be a useful parameter to predict OC accumulation potential in this region. Greater OC accumulation at sites THZZH-03 and THZZH-12 was likely caused by higher accretion rates at these sites. OC accumulation was also negatively correlated with elevation, which suggests OC accumulation is greater at lower elevation sites. Variance in accumulation rates accounted for most of the variation in accretion rates among sites. Similarities among accretion and OC accumulation results may have been partially caused by the fact that accretion and OC accumulation were not independent of one another.

Additional research is needed to provide insight on the validity of calculated accretion and OC accumulation rates from this study and proper application of ^{210}Pb dating models on salt marshes in this region. Longer cores should be taken to ensure the 1963 and 1954 ^{137}Cs horizons are reached. This would allow the researcher to determine the accuracy of ^{210}Pb accretion rates and proper application of ^{210}Pb models by comparing the depths of calculated ^{210}Pb ages with the depths of 1963 and 1954 ^{137}Cs horizons. Additionally, this would allow for the independent comparison of accretion and accumulation. The effect of elevation on accretion and OC accumulation could be better understood by grouping sampling sites within tighter elevation ranges separated by specified increments. The effect of vegetation on accretion over the time period measured for this study would be difficult to determine unless historical data on vegetation composition were made available. Due to the apparent high accretion rates in this

system, it may be useful to apply a more short-term method to determine accretion and accumulation rates. One such method is the feldspar clay marker technique (Cahoon and Turner 1989). This method allows the researcher to measure the accretion or accumulation of soil over much shorter time intervals (e.g. days, weeks, months) and test the effect of vegetation density on accretion given the known vegetation density over the sampling period. Measuring relative sea level rise in the Liaohe Delta region may provide insight on the influence of subsidence on accretion. In future studies, it may also be useful to measure the OM and OC composition of the suspended sediment load in tidal waters to determine if suspended sediment is the primary source of OM in this system.

REFERENCES

Ali, A. A., B. Ghaleb, M. Garneau, H. Asnong, and J. Loisel. 2008. Recent peat accumulation rates in minerotrophic peatlands of the Bay James region, Eastern Canada, inferred by ^{210}Pb and ^{137}Cs radiometric techniques. Applied Radiation and Isotopes. 66:1350–1358.

Anisfeld, S. C., M. J. Tobin, and G. Benoit. 1999. Sedimentation rates in flow-restricted and restored salt marshes in Long Island Sound, Estuaries. 22:231–244.

Appleby, P. G. and F. Oldfield. 1978. The calculation of Lead-210 dates assuming a constant rate of supply of unsupported ^{210}Pb to the sediment. Catena. 5:1–8.

Appleby, P. G. and F. Oldfield. 1983. The assessment of ^{210}Pb data from sites with varying sediment accumulation rates. Hydrobiologia. 103:29–35.

Aselmann, I., and P. J. Crutzen. 1989. Global distribution of natural freshwater wetlands and rice paddies, their net primary productivity, seasonality and possible methane emissions. Journal of Atmospheric Chemistry. 8:307–358.

Bao, K., H. Zhao, W. Xing, X, Lu, N. B. McLaughlin, and G. Wang. 2011. Carbon accumulation in temperate wetlands of Sanjiang Plain, Northeast China. Soil Science Society of America Journal. 75:2386–2397.

Baoshan, C., H. Qiang, and Z. Xinsheng. 2008. Ecological thresholds of *Suaeda salsa* to the environmental gradients of water table depth and soil salinity. Acta Ecologica Sinica. 28:1408–1418.

Batjes, N. H. 1996. Total carbon and nitrogen in the soils of the world. European Journal of Soil Science. 47:151–163.

Beerling, D., R. A. Berner, F. D. Mackenzie, M. B. Harfoot, and J. A. Pyle. 2009. Methane and the CH_4-related greenhouse effect over the past 400 million years. American Journal of Science. 309:97–113.

Benninger, L. K., D. M. Lewis, and K. K. Turekian. 1975. The use of natural Pb-210 as a heavy metal tracer in the river-estuarine system. In: T. M. Church (ed.) Marine Chemistry in the Coastal Environment, American Chemical Society Symposium Series 18. Washington, D.C. 202–210.

Bradley, P. M. and J. T. Morris. 1990. Influence of oxygen and sulfide concentration on nitrogen uptake kinetics in Spartina alterniflora. Ecology. 71:282–287.

Bradley, P. M. and J. T. Morris. 1992. Effect of salinity on the critical nitrogen concentration of *Spartina alterniflora* Loisel. Aquatic Botany. 43:149–161.

Boesch, D. F., M. N. Josselyn, A. J. Mehta, J. T. Morris, W. K. Nuttle, C. A. Simestad, and D. J. P. Swift. 1994. Scientific assessment of coastal wetland loss, restoration and management in Louisiana. Journal of Coastal Research. Special Issue No. 20:1–103.

Cahoon, D. R. and R. E. Turner. 1989. Accretion and canal impacts in a rapidly subsiding wetland II. Feldspar marker horizon technique. Estuaries. 12:260–268.

Cahoon, D. R. and D. J. Reed. 1995. Relationships among marsh surface topography, hydroperiod, and soil accretion in a deteriorating Louisiana salt marsh. Journal of Coastal Research. 11:357–369.

Callaway, J. C., R. D. DeLaune, and W. H. Patrick Jr. 1998. Heavy metal chronologies in selected coastal wetlands from Northern Europe. Marine Pollution Bulletin. 36:82–96.

Campbell, B. L. 1983. Applications of environmental Caesium-137 for the determination of sedimnentation rates in reservoirs and lakes and related catchment studies in developing countries. Radioisotopes in sediment studies, I.A.E.A. Tech. Doc. 298:7–30.

Chmura, G. L., A. Coffey, and R. Crago. 2001. Variation in surface sediment deposition on salt marshes in the Bay of Fundy. Journal of Coastal Research. 17:221–227.

Chmura, G. L., S. C. Anisfeld, D. R. Cahoon, and J. C. Lynch. 2003. Global carbon sequestration in tidal, saline wetland soils. Global Biogeochemical Cycles. 17:1–12.

Coleman, N. T., R. J. Lewis, and D. Craig. 1963. Sorption of Cesium by soils and its displacement by salt solutions. Soil Science Society of America Proceedings. 27:290–294.

Collins, L. M., J. M. Collins, and L. B. Leopold. 1987. Geomorphic processes of an estuarine marsh: preliminary results and hypotheses. In: V. Gardiner (ed.). International geomorphology Part 1. John Wiley & Sons Ltd. Chichester. 1049–1072.

Connor, R. F., G. L. Chmura, and C. B. Beecher. 2001. Carbon accumulation in Bay of Fundy salt marshes: Implications for restoration of reclaimed marshes. Global Biogeochemical Cycles. 0:1–12.

Craft, C. B., E. D. Seneca, and S.W. Broome. 1991. Loss on ignition and Kjeldahl digestion for estimating organic carbon and total nitrogen in estuarine marsh soils: Calibration with Dry Combustion. Estuaries. 14:175–179.

Craft, C. B. and C. J. Richardson. 1993. Peat accretion and nitrogen, phosphorus and organic carbon accumulation in nutrient-enriched and unenriched Everglades peatlands. Ecological Applications. 3:446–458.

Craft, C. B. and C. J. Richardson. 1998. Recent and long-term organic soil accretion and nutrient accumulation in the Everglades. Soil Science Society of America Journal. 62:834–843.

DeLaune, R.D., W.H. Patrick Jr., R.J. Buresch. 1978. Sedimentation rates determined by ^{137}Cs dating in a rapidly accreting salt marsh. Nature. 275:532–533.

DeLaune, R. D., C. N. Reddy, and W. H. Patrick Jr. 1981a. Accumulation of plant nutrients and heavy metals through sedimentation processes and accretion in a Louisiana salt marsh. Estuaries. 4:328–334.

DeLaune, R. D., C. N. Reddy, and W. H. Patrick Jr. 1981b. Organic matter decomposition in soil as influenced by pH and redox conditions. Soil Biology and Biochemistry. 13:533–534.

DeLaune, R. D., C. J. Smith, and W. H. Patrick Jr. 1983. Methane release from Gulf coast wetlands. Tellus. 35B:8–15.

Dring, M. J. 1982. The biology of marine plants. Edward Arnold. London.

Duning, L., L. Xinghen, H. Yuanman, and W. Xianli. 1996. Protection of littoral wetlands in North China, ecological and environmental characteristics. Ambio. 25:2–5.

Eakins, J.D. 1982. The ^{210}Pb technique for dating sediments, and some applications. AAEC Research Establishment, Lucas Heights Research Laboratories, PMB Sutherland, 3322, N.S.W., Australia. 30–47.

Euliss, N. H., R. A. Gleason, A. Olness, R. L. McDougal, H. R. Murkin, R. D. Robarts, R. A. Bourbonniere, and B. G. Warner. 2006. North American prairie wetlands are important nonforested land-based carbon storage sites. Science of the Total Environment. 361:179–188.

French, J. 2006. Tidal marsh sedimentation and resilience to environmental change: Exploratory modelling of tidal, sea-level and sediment supply forcing in predominantly allochthonous systems. Marine Geology. 235:119–136.

Fu, X., F. Wang, and H. Wang. 2011. Analysis of estuarine and coastal pollution of Bohai. International Conference on Bioinformatics and Biomedical Engineering. Wuhan. 1–4.

Gambrell, R. P. 1994. Trace and toxic metals in wetlands–A review. Journal of Environmental Quality. 23:883–891.

Gorham, E. 1991. Northern peatlands: Role in the carbon cycle and probable responses to climatic warming. Ecological Applications. 1:182–195.

Guo, W., M. He, Z. Yang, C. Lin, X. Quan, and H. Wang. 2007. Distribution of polycyclic aromatic hydrocarbons in water, suspended particulate matter and sediment from Daliao River watershed, China. Chemosphere. 68:93–104.

He, Q. and D. E. Walling. 1996. Interpreting particle size effects in the adsorption of ^{137}Cs and unsupported ^{210}Pb by mineral soils and sediments. Journal of Environmental Radioactivity. 30:117–137.

Hensel, P. F., J. W. Day Jr., and D. Pont. 1999. Wetland vertical accretion and soil elevation change in the Rhone River Delta, France: The importance of riverine flooding. Journal of Coastal Research. 15:668–681.

Howes, B. L., J. W. H. Dacey, and J. M. Teal. 1985. Annual carbon mineralization and belowground production of *Spartina alterniflora* in a New England salt marsh. Ecology. 66:595–605.

Howes, B. L., J. W. H. Dacey, and D. D. Goehringer. 1986. Factors controlling the growth form of *Spartina alterniflora*: Feedbacks between aboveground production, sediment oxidation, nitrogen, and salinity. Journal of Ecology. 74:881–898.

Ji, Y.H., G.S. Zhou, G.H. LV, X.L. Zhao, and Q.Y. Jia. 2009. Expansion of *Phragmites australis* in the Liaohe Delta, north-east China. Weed Research. 49:613–620.

Jusi, W. 1989. Water pollution and water shortage problems in China. Journal of Applied Ecology. 26:851–857.

Kingsbury, R. W. and E. Epstein. 1986. Salt sensitivity in wheat: A case for specific ion toxicity. Plant Physiology. 80:651–654.

Koch, M. S. and I. A. Mendelssohn. 1989. Sulphide as a soil phytotoxin: differential responses in two marsh species. Journal of Ecology. 77:565–578.

Koch, M. S., I. A. Mendelssohn, and K. L. McKee. 1990. Mechanism for the hydrogen sulfide-induced growth limitation in wetland macrophytes. Limnology and Oceanography. 35:399–408.

Koide, M. and K. W. Bruland. 1975. The electrodeposition and determination of radium by isotopic dilution in sea water and in sediments simultaneously with other natural radionuclides. Analytica Chimica Acta. 75:1–19.

Lehner, B. and P. Doll. 2004. Development and validation of a global database of lakes, reservoirs, and wetlands. Journal of Hydrology. 296:1–22.

Li, X., X. Song, Y. Zheng, and B. Harmsb. 2010. Wetland mitigation and its ecological consequences for endangered waterbirds in the Liaohe River Delta wetlands, China. In:

2010 International Conference on Mechanic Automation and Control Engineering. Institute of Electrical and Electronics Engineers, Red Hook, NY. 1691–1700.

Liu, Z., H. Liu, and X. Lu. 2000. Study on wetland resources in deltas around Bohai Sea. Chinese Geographical Science. 10:151–158.

Liu, Y. L., B. Zhang, C. L. Li, F. Hu, and B. Velde. 2008a. Long-term fertilization influences on clay mineral composition and ammonium adsorption in a rice paddy soil. Soil Science Society of America Journal. 72:1580–1590.

Liu, C., J. Sui, and Z. Wang. 2008b. Sediment load reduction in Chinese rivers. International Journal of Sediment Research. 23:44–55.

Liu, Z., S. Pan, X. Liu, and J. Gao. 2010. Distribution of ^{137}Cs and ^{210}Pb in sediments of tidal flats in north Jiangsu Province. Journal of Geographical Sciences. 20:91–108.

Liu, B., K. Hu, Z. Jiang, F. Qu, and X. Su. 2011. A 50-year sedimentary record of heavy metals and their chemical speciations in the Shuangtaizi River estuary (China): implications for pollution and biodegradation. Frontiers of Environmental Science and Engineering in China. 5:435–444.

Lomenick, T. F. and T. Tamura. 1965. Naturally occurring fixation of Cesium-137 on sediments of lacustrine origin. Soil Science Society of America Proceedings 1965. 383–387.

Mahall, B. E. and R. B. Park. 1976. The ecotone between *Spartina foliosa* trin. and *Salicornia virginica* l. in salt marshes of northern San Francisco Bay. Journal of Ecology. 64:793–809.

Marinucci, A. C., J. E. Hobbie, and J. V. K. Helfrich. 1983. Effect of litter nitrogen on decomposition and microbial biomass in *Spartina alterniflora*. Microbial Ecology. 9:27–40.

McCaffrey, R. J. and J. Thomson. 1980. A record of the accumulation of sediment and trace metals in a Connecticut salt marsh. Advances in Geophysics. 22:165–236.

McKee, K. L. and E. D. Seneca. 1982. The influence of morphology in determining the decomposition of two salt marsh macrophytes. Estuaries. 5:302–309.

McLatchey, G. P. and K. R. Reddy. 1998. Regulation of organic matter decomposition and nutrient release in a wetland soil. Journal of Environmental Quality. 27:1268–1274.

Melillo, J. M., J. D. Aber, and J. F. Muratore. 1982. Nitrogen and lignin control of hardwood leaf litter decomposition dynamics. Ecology. 63:621–626.

Mitsch, W. J. and X. Wu. 1995. Wetlands and Global Change. In R. Lal, J. Kimble, E. Levine, and B. A. Stewart, eds. Advances in Soil Science, Soil Management, and Greenhouse Effect. CRC Press/Lewis Publishers, Boca Raton, FL. 205–230.

Mitsch, W. J. and J. G. Gosselink. 2007. Wetlands. John Wiley & Sons, Inc. Hoboken, New Jersey.

Morris, J. T. 2007. Ecological engineering in intertidal salt marshes. Hydrobiologia. 577:161–168.

Morton, R. A., N. A. Buster, and M. D. Krohn. 2002. Subsurface controls on historical subsidence rates and associated wetland loss in Southcentral Louisiana. Gulf Coast Association of Geological Transactions. 52:767–778.

Nyman, J. A., R. D. DeLaune, W. H. Patrick Jr. 1990. Wetland soil formation in the rapidly subsiding Mississippi River Deltaic Plain: mineral and organic matter relationships. Estuarine Coastal and Shelf Science. 31:57–69.

Nyman, J. A. and R. D. DeLaune. 1991. CO_2 emission and soil Eh response to different hydrological conditions in fresh, brackish, and saline marsh soils. Limnology and Oceanography. 36:1406–1414.

Nyman, J. A., R. H. Chabreck, R. D. DeLaune, and W. H. Patrick Jr. 1993a. Submergence, salt-water intrusion, and managed Gulf coast marshes. In: Magoon, O.T., W.S.Wilson, H. Converse, and L.T. Tobin. (Eds). Coastal Zone '93: Proceedings of the Eighth Symposium on Coastal and Ocean Management, 19–23 July 1993, New Orleans, LA, American Society of Civil Engineers, New York. 1690–1704.

Nyman, J. A., R. D. DeLaune, H. H. Roberts, and W. H. Patrick Jr. 1993b. Relationship between vegetation and soil formation in a rapidly submerging coastal marsh. Marine Ecology Progress Series. 96:269–279.

Nyman, J. A., R. J. Walters, R. D. Delaune, and W. H. Patrick Jr. 2006. Marsh vertical accretion via vegetative growth. Estuarine Coastal and Shelf Science. 69:370–380.

Oenema, O. and R. D. DeLaune. 1988. Accretion rates in salt marshes in the Eastern Scheldt, south-west Netherlands. Estuarine Coastal Shelf Science. 26:379–394.

Ogrinc, N., G. Fontolan, J. Faganeli, and S. Covelli. 2005. Carbon and nitrogen comparisons of organic matter in coastal marine sediments (the Gulf of Trieste, N Adriatic Sea): indicators of sources and preservation. Marine Chemistry. 95:163–181.

Oldfield, F. and P. G. Appleby. 1984. Empirical testing of ^{210}Pb-dating models for lake sediments. In: Haworth, E. Y. and J. W. G. Lund (Ed.). Lake Sediments and Environmental History. The University of Minnesota Press. Minneapolis, MN. 93–124.

Orson, R. A., R. S. Warren, and W. A. Niering. 1998. Interpreting sea level rise and rates of vertical marsh accretion in a southern New England tidal salt marsh. Estuarine, Coastal and Shelf Science. 47:419–429.

Pennington, W., R. S. Cambray, and E. M. Fisher. 1973. Observations on lake sediments using fallout ^{137}Cs as a tracer. Nature. 242:324–326.

Rama, M. K. and E. D. Goldberg. 1961. Lead-210 in natural waters. Science. 134:98–99.

Reddy, K. R. and R. D. DeLaune. 2008. Biogeochemistry of Wetlands: Science and Applications. CRC Press. Boca Raton, FL. 447–476.

Reed, Denise J. 1989. Patterns of sediment deposition in subsiding coastal salt marshes, Terrebonne Bay, Louisiana: the role of winter storms. Estuaries. 12:222–227.

Reed, D. J. 1990. The impact of sea-level rise on coastal salt marshes. Progress in Physical Geography. 14:465–476.

Reed, D. J. 1995. The response of coastal marshes to sea-level Rise: survival or submergence. Earth Surface Processes and Landforms. 20:39–48.

Rejmanek, M., C.E. Sasser, G.W. Peterson. 1988. Hurricane induced gulf coast sediment deposition in a gulf coast marsh. Estuarine Coastal and Shelf Science. 27:217–222.

Ritchie, J.C., and J.R. McHenry. 1990. Application of radioactive fallout cesium-137 for measuring soil erosion and sediment accumulation rates and patterns: a review. Journal of Environmental Quality. 19:215–233.

Robbins, J. A. and D. N. Edgington. 1975. Determination of recent sedimentation rates in Lake Michigan using Pb-210 and Cs-137. Geochimica et Cosmochimica Acta. 39:285–304.

Robbins, J. A. 1978. Geochemical and geophysical applications of radioactive lead. In: Nriagu, J.O. (Ed.). The Biogeochemistry of Lead in the Environment. Elsevier/North-Holland Biomedical Press. Amsterdam, The Netherlands. 285–393.

Robterts, H. H. 1997. Dynamic changes of the Holocene Mississippi River delta plain: the delta cycle. Journal of Coastal Research. 13:605–627.

Rooth, J.E. and J.C. Stevenson. 2000. Sediment deposition patterns in *Phragmites australis* communities: Implications for coastal areas threatened by rising sea-level. Wetlands Ecology and Management. 8:173–183.

Rooth, J. E., J. C. Stevenson, and J. C. Cornwall. 2003. Increased sediment accretion rates following invasion by *Phragmites australis*: The role of litter. Estuaries. 26:475–483.

Roulet, N. T. 2000. Peatlands, carbon storage, greenhouse gases, and the Kyoto Protocol: Prospects and significance for Canada. Wetlands. 20:605–615.

Scott, D. A. 1989. A directory of Asian wetlands. IUCN, ICBP & IWRB, Cambridge University Press, Cambridge UK. 129–294.

Sedlacek, J., F. Sebesta, and P. Benes. 1980. Scintillation of emanometric determination of Radium-226 in waters using a new method of Radium preconcentration. Journal of Radioanalytical Chemistry. 59:45–53.

Smart, R. M. and J. W. Barko. 1980. Nitrogen nutrition and salinity tolerance of *Distichlis spicata* and *Spartina alterniflora*. Ecology. 61:630–638.

Sokal, Robert R., and F. James Rohlf. 1995. Biometry, The Principles and Practice of Statistics in Biological Research, 3rd ed. W. H. Freeman and Company, New York, NY.

Staunton, S. and M. Roubaud. 1997. Adsorption of ^{137}Cs on montmorillonite and illite: effect of charge compensating cation, ionic strength, concentration of Cs, K, and fulvic acid. Clays and Clay Minerals. 45:251–260.

Temmerman, S., G. Govers, S. Wartel, P. Meire. 2004. Modelling estuarine variations in tidal marsh sedimentation: response to changing sea level and suspended sediment concentrations. Marine Geology. 212:1–19.

Turner, R. E., E. M. Swenson, C. S. Milan, and J. M. Lee. 2007. Hurricane signals in salt marsh sediments: Inorganic sources and soil volume. Limnology and Oceanography. 52:1231–1238.

Valiela, I., J. M. Teal, S. D. Allen, R. V. Etten, D. Goehringer, and S. Volkmann. 1985. Decomposition in salt marsh ecosystems: the phases and major factors affecting disappearance of above-ground organic matter. Journal of Experimental Marine Biology and Ecology. 89:29–54.

Wan, L., N. B. Wang, Q. B. Li, Z. C. Zhou, B. Sun, K. Xue, Z. Q. Ma, J. Tian, and N. Du. 2008. Estival distribution of dissolved metal concentrations in Liaodong Bay. Bulletin of Environmental Contamination and Toxicology. 80:311–314.

Wang, A., S. Gao, J. Jia, and S. Pan. 2005. Sedimentation rates in Wanggang salt marshes, Jiangsu. Journal of Geographical Sciences. 15:199–209.

White, D. A. and J. M. Trapani. 1982. Factors influencing disappearance of *Spartina alterniflora* from litterbags. Ecology. 63:242–245.

Whiting, G. J. and J. P. Chanton. 2001. Greenhouse carbon balance of wetlands: methane emission versus carbon sequestration. Tellus. 53B:521–528.

Wilson, J. O., I. Valiela, and T. Swain. 1986. Carbohydrate dynamics during decay of litter of *Spartina alterniflora*. Marine Biology. 92:277–284.

Windham, L. 2001. Comparisons of biomass production and decomposition between *Phragmites australis* (common reed) and *Spartina patens* (salt hay grass) in brackish tidal marshes of New Jersey, USA. Wetlands. 21:179–188.

Wolaver, T. G., R. F. Dame, J. D. Spurrier, and A. B. Miller. 1988. Sediment exchange between a euhaline salt marsh in South Carolina and the adjacent tidal creek. Journal of Coastal Research. 4:17–26.

Wolff, W. J., M. J. Van Eeden, and E. Lammens. 1979. Primary production and import of particulate organic matter on a salt marsh in the Netherlands. Netherlands Journal of Sea Research. 13:242–255.

Xu, B., X. Yang, Z. Gu, Y. Zhang, Y. Chen, and Y. Lv. 2009. The trend and extent of heavy metal accumulation over last one hundred years in the Liaodong Bay, China. Chemosphere. 75:442–446.

Xue, Y., Y. Zhang, S. Ye, J. Wu, and Q. Li. 2005. Land subsidence in China. Environmental Geology. 48:713–720.

Yang, S. and J. Chen. 1995. Coastal salt marshes and mangrove swamps in China. Chinese Journal of Oceanology and Limnology. 13:318–324.

Zhang, J and C. L. Liu. 2002. Riverine composition and estuarine geochemistry of particulate metals in China–weathering features, anthropogenic impact and chemical fluxes. Estuarine, Coastal and Shelf Science. 54:1051–1070.

APPENDIX I. SOIL CORING DEVICE

APPENDIX II: INSTRUMENTS AND PRECISIONS

Instrument Descriptions			
Instrument	**Brand**	**Model**	**Additional Information**
Small scale (for LOI determinations)	Mettler Toledo	XS205 dual range	Max wt. 81 g/220 g, d=0.01 mg/0.1 mg
Large scale (for sample counting prep)	Mettler Toledo	PL3001-S.	Max wt. 3100 g, d=0.1 g
Drying oven (for drying at 105^{o} C)	SANFA	DHG-9202-(2SA)	
Combustion muffle furnace	Beijing Pyramid Technology		
Lab pH meter	Mettler Toledo	Seven Multi pH	
Lab pH electrode	Mettler Toledo	413 pH electrode	
Laser particle analyzer	Malvern	Mastersizer 2000	
Broad Energy Ge Detector	Canberra	BE3830	Typical Rel. efficiency: ≥ 34%

APPENDIX III: BD, OM, IM, AND OC

Core ID	Sample #	Mid Depth (cm)*	BD (g cm^{-3})*	OM (%)	Min (%)	OC (%)
THZZH-12	51	1.26	1.14	2.91	97.09	1.17
	51	1.26		2.77	97.23	1.11
	52	3.77	1.18	3.18	96.82	1.27
	53	6.29	1.22	2.83	97.17	1.13
	54	8.80	1.16	3.42	96.58	1.37
	55	11.32	1.25	3.42	96.58	1.37
	56	13.84	1.32	3.60	96.40	1.44
	57	16.35	1.17	3.82	96.18	1.53
	58	18.87	1.22	3.90	96.10	1.56
	59	21.38	1.21	3.81	96.19	1.53
	60	23.90	1.13	3.99	96.01	1.60
	61	26.41	1.25	3.81	96.19	1.53
	62	28.93	1.30	3.19	96.81	1.28
	63	31.45	1.17	3.06	96.94	1.23
	64	33.96	1.26	3.09	96.91	1.24
	65	36.48	1.25	3.70	96.30	1.48
	66	38.99	1.26	3.19	96.81	1.28
	67	41.51	1.25	3.70	96.30	1.48
	68	44.02	1.30	3.12	96.88	1.25
	68	44.02		2.96	97.04	1.19
	69	46.54	1.24	2.75	97.25	1.10
	70	49.05	1.13	2.84	97.16	1.14
	71	51.57	1.18	3.17	96.83	1.27
	72	54.09	1.16	3.02	96.98	1.21
	73	56.60	1.26	2.83	97.17	1.13
	74	59.12	1.19	2.50	97.50	1.00
	75	61.63	1.18	2.54	97.46	1.02
	76	64.15	1.19	2.81	97.19	1.13
	77	66.66	0.91	2.73	97.27	1.10
	78	69.18	1.11	3.12	96.88	1.25
	79	71.70	1.07	2.56	97.44	1.03
	80	74.21	1.44	2.57	97.43	1.03
	80	74.21		2.57	97.43	1.03
	81	76.73	1.15	2.62	97.38	1.05
	82	78.99	1.12	2.68	97.32	1.07

*Values adjusted for compaction

Core ID	Sample #	Mid Depth (cm)*	BD (g cm^{-3})*	OM (%)	Min (%)	OC (%)
THZZH-06	20	1.31	1.02	3.87	96.13	1.55
	20	1.31		3.83	96.17	1.54
	21	3.92	1.02	3.33	96.67	1.34
	22	6.53	1.45	3.43	96.57	1.37
	23	9.15	1.24	3.53	96.47	1.42
	24	11.76	1.14	3.78	96.22	1.52
	25	14.37	1.36	3.40	96.60	1.36
	26	16.98	1.33	3.42	96.58	1.37
	27	19.60	1.31	3.53	96.47	1.42
	27	19.60		3.56	96.44	1.43
	28	22.21	1.32	3.45	96.55	1.39
	29	24.82	1.30	3.67	96.33	1.47
	30	27.44	1.15	3.29	96.71	1.32
	31	30.05	1.24	3.05	96.95	1.22
	32	32.66	1.33	2.93	97.07	1.18
	33	35.27	1.28	3.00	97.00	1.20
	34	37.89	1.28	3.15	96.85	1.26
	35	40.50	1.29	3.00	97.00	1.20
	36	43.11	1.37	2.93	97.07	1.18
	37	45.73	1.44	2.73	97.27	1.09
	37	45.73		2.76	97.24	1.11
	38	48.34	1.42	2.73	97.27	1.09
	39	50.95	1.32	2.78	97.22	1.11
	40	53.56	1.46	2.64	97.36	1.06
	41	56.18	1.36	2.81	97.19	1.13
	42	58.79	1.39	2.92	97.08	1.17
	43	61.40	1.41	2.54	97.46	1.02
	44	64.02	1.37	2.27	97.73	0.91
	45	66.63	1.47	2.83	97.17	1.14
	46	69.24	1.48	2.94	97.06	1.18
	47	71.85	1.46	2.89	97.11	1.16
	47	71.85		2.91	97.09	1.17
	48	74.47	1.49	2.97	97.03	1.19
	49	77.08	1.51	2.99	97.01	1.20
	50	78.69	1.31	3.47	96.53	1.39

*Values adjusted for compaction

Core ID	Sample #	Mid Depth (cm)	BD (g cm^{-3})	OM (%)	Min (%)	OC (%)
THZZH-04	83	1.25	1.20	4.12	95.88	1.65
	83	1.25		4.54	95.46	1.82
	84	3.75	0.96	3.85	96.15	1.55
	85	6.25	1.03	3.95	96.05	1.59
	86	8.75	0.98	3.93	96.07	1.58
	87	11.25	0.94	3.80	96.20	1.53
	88	13.75	1.13	3.73	96.27	1.50
	89	16.25	1.03	2.90	97.10	1.16
	90	18.75	0.97	3.12	96.88	1.25
	90	18.75		3.23	96.77	1.30
	91	21.25	1.20	3.07	96.93	1.23
	92	23.75	1.22	2.91	97.09	1.17
	93	26.25	1.20	2.98	97.02	1.20
	94	28.75	1.24	2.98	97.02	1.19
	95	31.25	1.23	2.75	97.25	1.10
	96	33.75	1.30	2.69	97.31	1.08
	97	36.25	1.17	2.75	97.25	1.10
	98	38.75	1.30	2.55	97.45	1.02
	99	41.25	1.27	2.45	97.55	0.98
	100	43.75	1.27	2.43	97.57	0.97
	100	43.75		2.34	97.66	0.94
	101	46.25	1.30	2.10	97.90	0.84
	102	48.75	1.32	2.21	97.79	0.88
	103	51.25	1.55	2.66	97.34	1.07
	104	53.75	1.56	2.00	98.00	0.80
	105	56.25	1.30	2.08	97.92	0.83
	106	58.75	1.58	1.77	98.23	0.71
	107	61.25	1.36	1.80	98.20	0.72
	108	63.75	1.34	1.72	98.28	0.69
	109	66.25	1.47	1.73	98.27	0.69
	110	68.75	1.45	1.69	98.31	0.68
	110	68.75		1.71	98.29	0.68
	111	71.25	1.36	1.69	98.31	0.68
	112	73.75	1.53	1.53	98.47	0.61
	113	76.25	1.48	1.64	98.36	0.66
	114	78.75	1.69	1.72	98.28	0.69

Core ID	Sample #	Mid Depth (cm)	BD (g cm^{-3})	OM (%)	Min (%)	OC (%)
THZZH-03	115	1.25	1.09	4.62	95.38	1.85
	116	3.75	0.97	4.25	95.75	1.71
	117	6.25	1.03	4.27	95.73	1.71
	118	8.75	1.22	4.00	96.00	1.60
	118	8.75		3.99	96.01	1.60
	119	11.25	1.12	3.96	96.04	1.59
	120	13.75	1.00	4.18	95.82	1.68
	121	16.25	0.97	4.29	95.71	1.72
	122	18.75	1.05	4.11	95.89	1.65
	123	21.25	1.07	4.05	95.95	1.63
	124	23.75	0.74	4.31	95.69	1.73
	124	23.75		4.19	95.81	1.68
	125	26.25	1.05	4.07	95.93	1.63
	126	28.75	1.14	4.05	95.95	1.62
	127	31.25	1.13	3.77	96.23	1.51
	128	33.75	1.13	3.79	96.21	1.52
	129	36.25	0.86	3.74	96.26	1.50
	130	38.75	1.02	3.68	96.32	1.48
	130	38.75		3.65	96.35	1.46
	131	41.25	1.06	3.73	96.27	1.50
	132	43.75	1.08	3.81	96.19	1.53
	133	46.25	0.97	3.78	96.22	1.52
	134	48.75	1.42	3.37	96.63	1.35
	135	51.25	1.04	3.22	96.78	1.29
	136	53.75	1.13	3.16	96.84	1.27
	137	56.25	1.22	3.04	96.96	1.22
	138	58.75	1.14	2.80	97.20	1.12
	139	61.25	1.24	2.91	97.09	1.17
	140	63.75	1.22	2.21	97.79	0.89
	141	66.25	1.09	2.33	97.67	0.93
	142	68.75	1.30	2.09	97.91	0.84
	143	71.25	1.31	2.42	97.58	0.97
	144	73.75	1.27	2.35	97.65	0.94
	145	76.25	1.43	2.56	97.44	1.02
	146	78.75	1.36	2.73	97.27	1.09

Core ID	Sample #	Mid Depth (cm)*	BD (g cm^{-3})*	OM (%)	Min (%)	OC (%)
THZZH-07	147	1.33	0.88	3.99	96.01	1.60
	148	4.00	1.18	3.54	96.46	1.42
	149	6.67	1.17	3.74	96.26	1.50
	150	9.33	1.19	3.54	96.46	1.42
	151	12.00	1.15	11.87	88.13	4.79
	152	14.67	1.16	3.28	96.72	1.32
	153	17.33	1.15	3.52	96.48	1.41
	154	20.00	1.15	3.26	96.74	1.31
	155	22.67	1.13	3.58	96.42	1.44
	156	25.33	1.16	3.20	96.80	1.29
	157	28.00	1.24	2.93	97.07	1.17
	158	30.67	1.30	3.48	96.52	1.40
	159	33.33	1.20	3.37	96.63	1.35
	160	36.00	1.22	3.55	96.45	1.42
	161	38.67	1.24	3.49	96.51	1.40
	162	41.33	1.15	2.89	97.11	1.16
	163	44.00	1.22	3.66	96.34	1.47
	164	46.67	1.35	2.82	97.18	1.13
	165	49.33	1.14	2.65	97.35	1.06
	166	52.00	1.16	2.86	97.14	1.15
	167	54.67	1.18	3.20	96.80	1.28
	168	57.33	1.15	3.20	96.80	1.28
	169	60.00	1.18	3.04	96.96	1.22
	170	62.67	1.07	3.94	96.06	1.58
	171	65.33	1.05	3.59	96.41	1.44
	172	68.00	1.26	3.40	96.60	1.36
	173	70.67	1.13	3.55	96.45	1.42
	174	73.33	1.15	3.74	96.26	1.50
	175	76.00	1.28	3.97	96.03	1.59
	176	78.67	1.02	4.07	95.93	1.63

*Values adjusted for compaction

Core ID	Sample #	Mid Depth (cm)*	BD (g cm^{-3})*	OM (%)	Min (%)	OC (%)
SKZH-11	1	1.42	0.93	3.48	96.52	1.40
	2	4.26	1.12	3.45	96.55	1.38
	3	7.11	1.11	3.53	96.47	1.41
	4	9.95	1.34	3.56	96.44	1.43
	5	12.79	1.19	3.45	96.55	1.38
	6	15.63	0.99	3.47	96.53	1.39
	7	18.47	1.05	3.70	96.30	1.49
	8	21.32	0.90	3.26	96.74	1.31
	9	24.16	0.86	3.36	96.64	1.35
	10	27.00	0.86	3.41	96.59	1.37
	11	29.84	1.09	3.27	96.73	1.31
	12	32.68	1.08	3.31	96.69	1.33
	13	35.53	1.05	2.84	97.16	1.14
	14	38.37	1.16	2.67	97.33	1.07
	15	41.21	1.12	2.83	97.17	1.14
	16	44.05	1.19	2.65	97.35	1.06
	17	46.89	1.20	2.52	97.48	1.01
	18	49.74	1.17	2.40	97.60	0.96
	19	52.08	1.30	2.62	97.38	1.05

*Values adjusted for compaction

Core ID	Sample #	Mid Depth (cm)*	BD (g cm^{-3})*	OM (%)	Min (%)	OC (%)
SKZH-10	206	1.41	1.18	3.65	96.35	1.46
	207	4.23	1.19	3.51	96.49	1.41
	208	7.05	1.04	3.50	96.50	1.40
	209	9.86	1.11	3.53	96.47	1.42
	210	12.68	0.97	3.59	96.41	1.44
	211	15.50	1.17	3.48	96.52	1.40
	212	18.32	1.06	3.52	96.48	1.41
	213	21.14	1.15	3.29	96.71	1.32
	214	23.95	1.24	3.05	96.95	1.22
	215	26.77	1.07	3.21	96.79	1.29
	216	29.59	1.23	3.21	96.79	1.29
	217	32.41	1.13	3.14	96.86	1.26
	218	35.23	1.30	3.16	96.84	1.27
	219	38.05	1.27	3.01	96.99	1.20
	220	40.86	1.10	3.07	96.93	1.23
	221	43.68	1.38	2.72	97.28	1.09
	222	46.50	1.25	2.89	97.11	1.16
	223	49.32	1.43	2.98	97.02	1.19
	224	52.14	1.18	3.20	96.80	1.28
	225	54.95	1.22	3.08	96.92	1.24
	226	57.77	1.15	2.96	97.04	1.19
	227	60.59	1.05	2.85	97.15	1.14

*Values adjusted for compaction

Core ID	Sample #	Mid Depth (cm)*	BD (g cm^{-3})*	OM (%)	Min (%)	OC (%)
SKZH-08	179	1.37	0.93	4.32	95.68	1.73
	180	4.11	1.09	4.00	96.00	1.61
	181	6.85	1.00	3.79	96.21	1.52
	182	9.59	1.04	3.66	96.34	1.47
	183	12.33	0.92	3.71	96.29	1.49
	184	15.07	1.01	3.85	96.15	1.54
	185	17.81	0.90	3.98	96.02	1.60
	186	20.56	0.96	3.99	96.01	1.60
	187	23.30	0.94	3.84	96.16	1.54
	188	26.04	1.01	3.59	96.41	1.44
	189	28.78	1.03	3.68	96.32	1.48
	190	31.52	1.10	3.70	96.30	1.48
	191	34.26	0.95	3.93	96.07	1.58
	192	37.00	1.04	3.87	96.13	1.55
	193	39.74	1.02	3.62	96.38	1.45
	194	42.48	0.99	3.65	96.35	1.46
	195	45.22	0.96	3.68	96.32	1.48
	196	47.96	0.86	3.80	96.20	1.52
	197	50.70	1.10	3.94	96.06	1.58
	198	53.44	1.01	3.66	96.34	1.47
	199	56.19	1.09	3.47	96.53	1.39
	200	58.93	0.87	3.34	96.66	1.34
	201	61.67	0.94	3.48	96.52	1.39
	202	64.41	0.94	3.57	96.43	1.43
	203	67.15	1.07	3.86	96.14	1.55
	204	69.89	0.90	3.63	96.37	1.46
	205	72.63	1.10	3.67	96.33	1.47

*Values adjusted for compaction

Core ID	Sample #	Mid Depth (cm)*	BD (g cm^{-3})*	OM (%)	Min (%)	OC (%)
SKZH-09	228	1.36	0.86	3.72	96.28	1.49
	229	4.09	0.88	3.77	96.23	1.51
	230	6.82	0.62	3.95	96.05	1.58
	231	9.55	0.83	3.98	96.02	1.59
	232	12.27	0.86	2.94	97.06	1.18
	233	15.00	0.98	3.24	96.76	1.30
	234	17.73	0.82	3.34	96.66	1.34
	235	20.45	0.85	3.46	96.54	1.39
	236	23.18	0.83	3.54	96.46	1.42
	237	25.91	0.82	3.70	96.30	1.48
	238	28.64	0.78	4.85	95.15	1.95
	239	31.36	0.85	4.86	95.14	1.95
	240	34.09	0.82	4.65	95.35	1.87
	241	36.82	0.84	4.74	95.26	1.90
	242	39.55	1.07	4.81	95.19	1.93
	243	42.27	0.78	4.92	95.08	1.97
	244	44.23	0.78	4.77	95.23	1.91
	245	47.73	0.90	4.73	95.27	1.90
	246	50.45	0.88	4.62	95.38	1.85
	247	53.18	0.98	4.43	95.57	1.78
	248	55.91	1.07	4.15	95.85	1.66
	249	58.64	1.20	3.89	96.11	1.56

*Values adjusted for compaction

VITA

Nicholas Lawrence Yuknis was born in Harvey, Illinois, in 1987. As a child growing up in Indiana, he thoroughly enjoyed the outdoors and took every opportunity to go hunting and fishing with his family around the country and near his home. Through his travels and experiences, he developed an appreciation for, and interest in environment science and management that has fueled his educational and professional aspirations throughout his life.

Upon graduating high school, he followed in his brother's footsteps and attended Indiana University, Bloomington, where he majored in environmental management. It was during his tenure at Indiana University that he became particularly interested in wetland science and the complex interrelated processes occurring within wetland systems. He received a Bachelor of Science in Public Affairs degree from the School of Public and Environmental Affairs at Indiana University in May 2009 and immediately took a position with an ecological consulting company in Chicago, where he worked for over a year restoring wetland, prairie, and forest habitats throughout the Midwest. However, his thirst for knowledge about wetland systems was not yet quenched; this lead him to pursue a Master of Science in Environmental Sciences with a minor in wetland science and management at Louisiana State University. After graduating, Nicholas hopes to apply the knowledge and experience he has gained to a fulfilling career in the field of wetland science and management.